

Chinese Society of Aeronautics and Astronautics & Beihang University

Chinese Journal of Aeronautics

cja@buaa.edu.cn www.sciencedirect.com



REVIEW

Internal surface finishing and roughness measurement: A critical review



Jiang GUO^{a,*}, Qikai LI^a, Pu QIN^a, Ankang YUAN^a, Mingyang LU^a, Xiaolong KE^b, Yicha ZHANG^c, Benny C.F. CHEUNG^d

Received 27 July 2024; revised 25 August 2024; accepted 6 November 2024 Available online 17 November 2024

KEYWORDS

Internal surface finishing; Roughness measurement; Small aperture; Complex structure; Tool-probing Abstract Modern industrial equipment is increasingly characterized by miniaturization, integration, and high performance, necessitating the production of complex structural parts with exceptionally high internal surface quality. Direct manufacturing often leads to high internal surface roughness, which traditional finishing and measuring methods cannot adequately address due to the decreasing size and increasing complexity of internal structures. This is especially true for components like pipes with large aspect ratios, extremely small deep holes, multi-stage bends, cross pipes, and array holes. To meet the high-performance manufacturing demands of these parts, advanced internal surface finishing and roughness measurement technologies have gained significant attention. This review focuses on the challenges and solutions related to internal surface parts with various apertures and complex structures. Internal surface finishing methods are categorized into mechanical finishing, fluid-based finishing, and energy-field-based finishing based on their characteristics. Roughness measurement technologies are divided into tool-probing and non-probing methods. The principles, required equipment, and key parameters of each finishing and measurement approach are discussed in detail. Additionally, the advantages and limitations of these methods are summarized, and future trends are forecasted. This paper serves as a comprehensive guide

E-mail address: guojiang@dlut.edu.cn (J. GUO).

Peer review under responsibility of Editorial Committee of CJA



Production and hosting by Elsevier

^a State Key Laboratory of High-performance Precision Manufacturing, Department of Mechanical Engineering, Dalian University of Technology, Dalian 116024, China

^b School of Mechanical and Automotive Engineering, Xiamen University of Technology, Xiamen 361024, China

^c Laboratoire d'Automatique de Mécanique et d'Informatique industrielles et Humaines, UMR 8201, CNRS, INSA Hauts-de-France, Univ. Polytechnique Hauts-de-France, 59313, Valenciennes, France

^d State Key Laboratory of Ultra-precision Machining Technology, Department of Industrial and Systems Engineering, The Hong Kong Polytechnic University, Hung Hom, Kowloon, Hong Kong

^{*} Corresponding author.

for researchers and engineers aiming to enhance the internal surface quality of complex structure parts.

© 2024 The Author(s). Published by Elsevier Ltd on behalf of Chinese Society of Aeronautics and Astronautics. This is an open access article under the CC BY-NC-ND license (http://creativecommons.org/licenses/by-nc-nd/4.0/).

1. Introduction

Internal surface quality is crucial to the performance of modern equipment, which aims for high efficiency, stability, and long service life. Due to increasing industrial demands, parts with high internal surface quality are widely used in various fields, such as aero-engines, automotive power systems, optical molds, biomedical devices, and semiconductor components, as shown in Fig. 1. The internal surface quality directly affects the fatigue strength and fit accuracy of parts, as well as the stability and flow resistance of contact media like air or fluids.^{1–3}

For instance, in an automobile engine, poor internal surface roughness of the cylinder can impact the matching state, leading to severe friction and air loss. In liquid delivery pipelines, such as oil pipes and needle tubes, high internal surface roughness can cause residue accumulation, potentially resulting in blockages. 4-6 In components handling high-speed fluids, such as intake passages and fuel nozzles, internal surface roughness affects the fluid's motion trajectory, influencing combustion efficiency.⁷ These applications generally require internal surface roughness at the submicron level or lower. In electronic devices and optical fibers used for communication, the demand for internal roughness reaches the nanometer level. Therefore, improving internal surface roughness is essential, especially in ultra-precision equipment. However, modern industry not only has stringent requirements for internal surface quality but also significantly increases the complexity of part structures to meet various working conditions.



Fig. 1 Applications of complex internal surface parts across various field.

Internal surface with complex structure generally contains the areas that are difficult to reach by using conventional tools. These structures typically feature small apertures, high depthto-diameter ratios, variable inner diameters, and multi-cross channels, etc. 9-11 For example, parts such as gun barrels and fuel spray rods often have depth-to-inner-diameter ratios above 50, while optical fiber preforms, medical needle tubes, and catheters can have ratios greater than 100. Recently, additive manufacturing technology has rapidly advanced, enabling the integrated molding of complex structures thanks to its high degree of freedom. 12 Additively manufactured cooling fins and tubes with the characteristics of multi-channel, multiintersection, and variable diameter have been applied in aviation, nuclear energy and other fields nowadays. 13 However, the internal surfaces of these parts are often quite poor due to stair-stepping effects, partially melted powders, and surface pores, with roughness typically exceeding ten microns, posing further challenges for internal surface finishing and measurement.1

Finishing complex surfaces with poor initial quality faces several challenges. The first is limited accessibility, as most existing high-efficiency, high-precision finishing technologies, such as single-point diamond turning and chemical mechanical polishing, are constrained by tool size and motion interference. The second challenge is low controllability. When using smallsized tools or free-flowing media, such as liquids or gases, to access internal areas of parts, how to achieve uniform materials removal within intricate internal structures is the main difficulty. For internal roughness measurement, limited accessibility is also the primary issue, which makes it challenging for high-precision measurement systems, typically requiring large equipment and complex optical configurations, to capture surface morphology accurately. When smaller equipment is used, maintaining measurement accuracy and stability then becomes the main challenge. Currently, a common method for internal surface measurement is to cut open the part. However, with rising manufacturing costs, this approach is gradually becoming less feasible.

In order to solve the above problems and realize sustainable manufacturing and test, researchers have developed a series of technologies according to the complexity of internal surface. In terms of finishing technology, researchers first optimized the size of the grinding tool, and combined with external field assistance such as electric and ultrasonic field, finished the surface by inserting the tool into the part. 15,16 However, with the increasing of the structure complexity, the mechanical method based on tool-probing cannot meet the requirements of accuracy and accessibility. As a result, the flexible finishing technology with the free movement of the processing medium has been widely used. For example, abrasive flow machining (AFM), ¹⁷ magnetic abrasive finishing (MAF), ¹⁸ electrochemical polishing (ECP)¹⁹ and so on. These technologies take advantage of the fluid or fluid-like nature of the processing medium that driven by external forces, such as pressure or

magnetic force. The medium moves deep into the internal space of the part and achieve material removal on the inner wall by mechanical scraping, impact or chemical corrosion, and finally to accomplish precision finishing process. In terms of internal surface quality measurement technologies, the researchers first miniaturized the stylus of contact measurement device, and has realized the roughness measurement of the 165 µm small hole of the fuel nozzle in 2000s.²⁰ In order to use optical method to achieve fast and efficient measurement of the hole surface, researchers optimized the size of optical circuit by means of built-in conical prisms and mirrors, and achieved high-precision and rapid measurement of 3 mm hole.²¹ With the increase of the depth-to-diameter ratio of the internal surface and the complexity of the structure, the optical fiber sensor and related measurement technology, which probes into the internal area with ultra-thin optical fibers to obtain the information of the scattered light, has also received extensive attention.

In recent years, the research focus on the internal finishing and related roughness measurement have developed a range of methods. But there are a few articles summarized these technologies based on the internal surface complexity and accessibility, which are the main concerns when the part has abnormal structure. Tan, et al.22 review the three nontraditional finishing methods of internal surface: AFM, MAF and fluidized bed machining (FBM), and summarized the principle, devices, main parameters, main applications of these three methods and introduced the variants of related technologies. Bedi, et al.²³ summarized and compare the finishing technologies for cylinder, including the griding, AFM and MAF. Lee, et al.²⁴ and Fang²⁵ reviewed the post-processing technologies suitable for additive manufacturing parts, then summarized and compared the advantages and disadvantages of various external and internal surface finishing technologies. In terms of internal surface roughness measurement methods. Peiner, et al.²⁶ compare the various tactile probing sensor for contour and roughness metrology with deep, narrow holes, and propose an extremely slender silicon cantilever for roughness measurements with narrow spray holes of advanced diesel injector nozzles. Jiao, et al.²⁷ review the non-destructive optical methods for the three-dimensional topography reconstruction and roughness measurement of inner wall, and compared the advantages and disadvantages of various optical methods in terms of calculation algorithms and optical circuit design. The summarization and conclusion of the above-mentioned reviews mostly focus on one or several representative technologies of internal surface, and seldom of them introduced a variety of complex structural parts. Moreover, to our best knowledge, seldom review article provide a summary of finishing and related roughness measurement method of internal surface at same time, though the measurement after finishing is actually a common trouble with a complex part.

In this paper, with the main thread of internal surface complexity, the finishing and related roughness measurement methods are reviewed from large to small diameter, from simple straight cylinder to elbow channel, variable diameter pipe, crossover tube, multi-way passage and other complicated structure. Firstly, inner surface finishing technologies are introduced, beginning with more established and conventional mechanical methods such as grinding and honing. Given the complexity of inner surface geometries, fluid-based finishing methods are subsequently discussed, including abrasive flow

machining and abrasive flow jet polishing. Finishing methods based on various energy fields, which address the limitations of traditional methods and offer new material removal principles, such as magnetic abrasive finishing and electrochemical polishing, are then presented. As shown in Fig. 2, the article then discusses internal surface measurement techniques, focusing on penetrating measurements for straight pipes, such as stylus, optical interference or scattering measurements, and replica film methods for curved pipes and the X-ray computed tomography (CT) method for complex structures. The principle, components, accuracy and efficiency of these technologies are presented, and the advantages and disadvantages of these technologies are compared. Finally, the summarization and prospects are provided, notably for the additively manufactured complex structure and extremely small-diameter structure that are still challengeable, to show readers a relatively comprehensive panorama of internal surface finishing and roughness measurement methods.

2. Internal surface finishing technology

Internal surface finishing technology refers to the method that utilizes tools or media to enter into the internal space of the part and realize micro material removal of inner wall. Generally, it could be divided into mechanical finishing and chemical finishing based on the removal mechanism. According to the complexity of internal passage, when finishing the internal surface of a middle-size straight pipe, the accessibility of the tool is significantly different from other complicated structures like elbow hole and irregular channel. So, in this section, internal surface finishing technologies are reviewed in three aspects: mechanical finishing, fluid-based finishing and energy-field-based finishing, which has developed rapidly in recent years.

2.1. Mechanical finishing

Mechanical finishing here is specified as the method of using tools mainly driven by motor to realize material removal. Traditional hole machining method such as turning, milling and boring cannot to applied to the finishing of internal surface due to the limitation of machining accuracy and efficiency. 28,29 Grinding, as a finishing method for rapidly converging surface roughness, can realize the finishing process of the internal surface of parts by controlling parameters such as grinding feed rate, grinding speed and grinding temperature.³⁰ It has been adapted to machining small holes nowadays by miniaturizing the grinding tool. Aurich, et al.31 developed a novel micro shaft grinding tool with cylindrical tool tip diameter between 13 μm and 100 μm, as shown in Fig. 3(b). The tool tip is electrically nickel plated with diamond grains of 1–3 µm to provide cutting edges and obtained low roughness in manufacture of microfluidic structure. Later in 2015, Aurich, et al.³² reduced the micro pencil grinding tool size to 4 µm diameter. Micro grinding tool are generally utilized for generating microstructures, and the method of grains coating includes electroplating, sintering, and chemical vapor deposition.

To further enhance the efficiency of small hole grinding, energy filed assistance was introduced into the process. Dong and Zhang³³ conducted experiments on grinding of ceramic materials with the aid of ultrasonic vibration. Compared to conventional grinding, the introduction of rotational ultra-

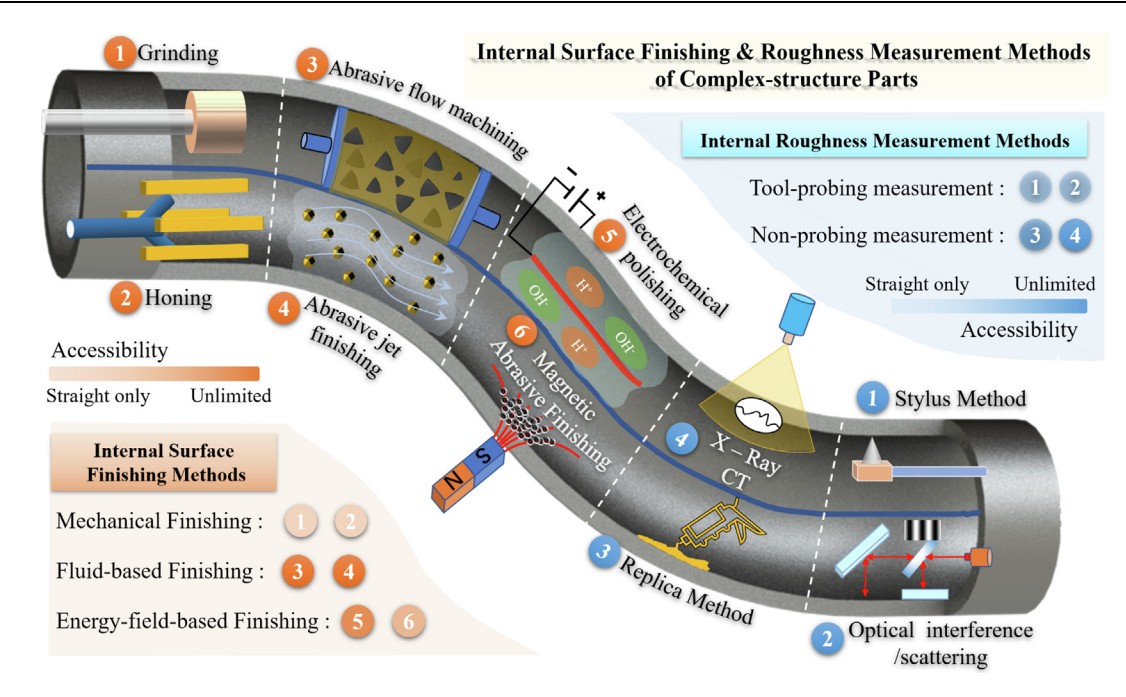


Fig. 2 Diagram of main internal surface finishing and roughness measurement methods for complex-structure parts.

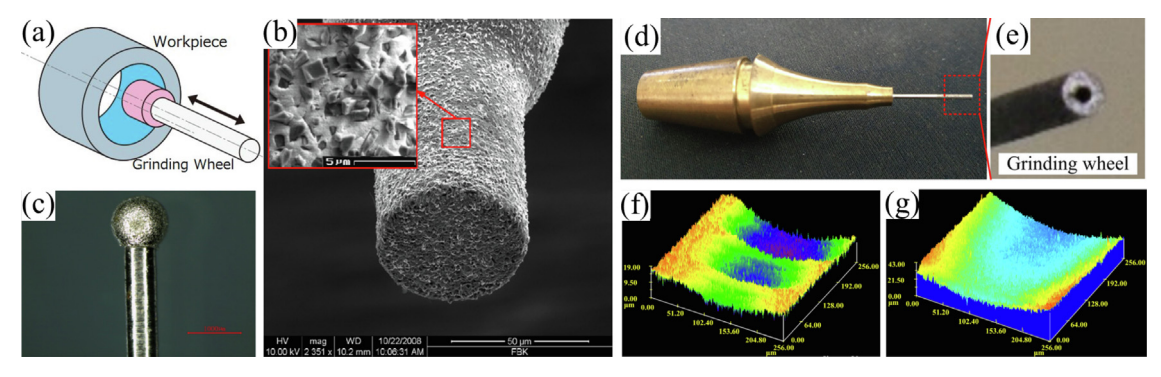


Fig. 3 (a) Schematic diagram of grinding; (b) SEM image of a micro pencil grinding tool³¹; (c) a small griding tool for electrolytic grinding³⁴; (d) grinding tool and (e) partial enlarged details, related workpiece topography (f) before and (g) after finishing.³³

sonic vibration significantly reduces friction between the diamond tool and the workpiece. Moreover, the debris generated during grinding is more effectively removed by the coolant. The improvements help to lower the heat generated and the grinding force required, thereby enhancing machining efficiency. By using an electroplated diamond grinding wheel with a diameter of 1 mm, the surface roughness of small holes with a depth of 1.2 mm was successfully reduced to 0.55 µm Ra. Zhu, et al.³⁴ developed an ultrasonic-assisted electrochemical drilling-grinding technique, involving the formation of a passivation film on the material surface through electrochemical reactions, which is then removed by mechanical grinding and ultrasonic vibration. The alternating use of electrochemical processing, mechanical grinding, and ultrasonic impact accelerates the renewal of the electrolyte in the machining gap and enhances the physical and chemical erosion of the material surface, finishing a 1.1 mm small hole and obtaining internal surface roughness of 0.31 µm Ra (Fig. 3(d-g)). Grinding can reduce internal roughness in a high rate, but improvement is limited by the burning and defects as a result of large amount

of cutting heat generated by the friction during high-speed grinding.

Honing can commonly achieve better surface quality and slightly improve the accuracy of the roundness of the internal surface. The finishing tool, called honing sticks or oilstone, is assembled on the honing spindle to make contact with internal surface and move in rotation and reciprocation. As shown in Fig. 4(a), the honing stone and the shaft are generally in a floating connection, and the pressure between oilstone and workpiece can be set to a certain value in a mechanical or hydraulic manner. Thus, the cutting force is relative constant, resulting in better surface quality. Honing is mostly used to finish boreholes larger than 5 mm, such as cylinders, holes in vales, connecting rod and case body. The depth to diameter ratio of the processed hole can reach ten or even larger, and the surface roughness after finishing can generally reach Ra 0.32–0.08 μm, even lower than 0.04 μm during fine honing.³⁵ Pan and Zhu³⁶ finished the Inconel 718 deep hole with 897.2 mm length and depth-diameter ratio larger than 10. Yang, et al.³⁷ developed a single-pass honing tool for a fuel

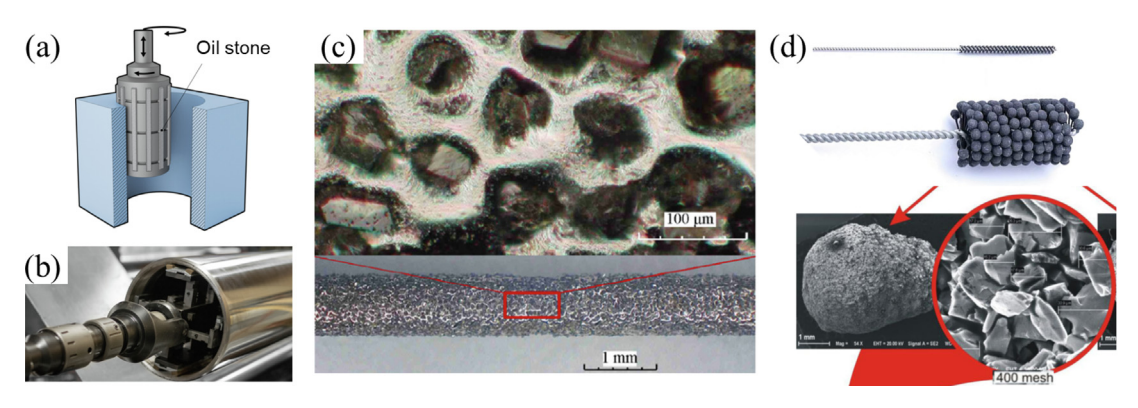


Fig. 4 (a) Schematic diagram and (b) equipment of honing; (c) small honing tool and enlarged details; (d) flexible honing tool and enlarged details.

nozzle with 0.75 mm diameter, the tool was dressed with CBN grains as shown in Fig. 4(c), the internal surface roughness obtained varying from 0.075 to 0.2 μ m Ra under different feed rate and retracting speed.

In these years, the flexible honing, where the abrasives and shaft are connected by flexible wire, has been widely used in finishing slender holes. The flex hone tool consists of a rigid metal rod, polymetric "bristles" with tips in the form of abrasive globules, which are arranged in a brush format. The abrasive type of flex hone tool usually are silicon carbide and aluminum oxide, and the size of abrasive grain can vary from 20 to 800 μ m. Comparison between conventional honing and flexible honing was investigated by Luciano José, they found the average values of area valleys and peaks were significantly reduced by 61% and 63% respectively through flexible honing. The materials of flexible honing tools can also be nylon in some cases where it serves as an auxiliary tool to enhance the materials remove.

Generally speaking, the mechanical finishing tool, driven by the spindle, can rotate at high speed and quickly removes the internal surface material of the workpiece. With the ability to rapidly improve the roughness to a certain range, mechanical finishing is the mainstream method in processing the parts that are accessible. However, the processing heat, which is prone to defects such as burns and residual stress that deteriorates the surface quality, has limited the applicability. Furthermore, the rigid shaft determines the mechanical finishing method is only suitable for straight tube. To finish internal structure with small size and large depth-to-diameter ratio, or bent passage, medium with higher flexibility is needed.

2.2. Fluid-based finishing

Fluid-based finishing (FBF) methods refer to those techniques that utilize the free abrasives to realize material removal based on the fluid or solid-like medium, which can arrive any internal corner of complex structure. As the viscosity decreases from high to low, the medium can be categorized into three types: solid-like medium, liquid, and air. These correspond to abrasive flow machining, abrasive jet finishing, and fluidized bed polishing, respectively. In most case, the complex internal structures are designed to transfer the fluid or air, so the FBF method could overcome the defects of mechanical finishing techniques and obtain the highest freedom degree in internal surface finishing.

2.2.1. Abrasive flow machining

AFM, also known as Extrude Honing, was originally developed by American Extrude Hone Corporation in the 1960 s for cylinder deburring. This technology employs the viscoelastic medium to carry abrasive particles in motion through areas such as workpiece surfaces, edges and channels under high pressure. It is a micro-cutting precision finishing technique that uses the scraping action of its abrasive grains to polish, deburr and chamfer the surface of the workpiece. As shown in Fig. 5(a). Under the high pressure of the piston, a fluid-like finishing abrasive containing abrasive particles reciprocates across the internal surface of the workpiece to remove material. By designing different types of fixtures, abrasive flow machining can deal with a wide range of complex internal surface parts. 42–47

AFM can be used to polish pipes with diameters varying from millimeters to decimeters. Singh and Sankar ⁴² used abrasive flow technology to polish 304 stainless steel with a diameter of 13 mm, reducing the inner surface roughness from 0.46 μm to 0.26 μm . To improve the removal efficiency, the author realized the finishing of 0.44 mm micro-slots by improving the abrasive medium and increasing the rheological shear force, which greatly increased the roughness (94%), from the original 3.54 μm roughness to 0.21 μm^{43} (Fig. 5(b)). Liu, et al. ⁴⁴ used the self-developed abrasive flow medium to polish the diesel engine nozzle, which has large hole diameter of 4 mm and small hole diameter of 0.16 mm, and found that the AFM process had the best effect when the abrasive concentration was 10% and the particle size was 6 μm , and the surface roughness could reach 0.496 μm .

In addition to simple straight pipes, abrasive flow can also polish various complex structures such as stepped pipes, bent pipes, cooling channels, and branch structures. Li, et al. 45 polished the fourth-order variable diameter pipe with solid–liquid two-phase abrasive flow, reducing the surface roughness *Ra* of the pipe from 1.469 μm to 0.295 μm after finishing. Han, et al. 46 studied the surface finish of SLM-fabricated conformal channels using abrasive flow machining. Seven types of internal cooling channels with a diameter of about 3 mm were fabricated in the bar using SLM technology. Under the same extrusion pressure of 80 bar, the internal channels were polished ten times through AFM media (ULV50%-54). The *Sa* of the surface of the conformal cooling slot was reduced from 7–9 μm to around 2 μm (Fig. 5g). Li et al. 45 used AFM to polish the S-shaped elbow with side openings and optimized the process

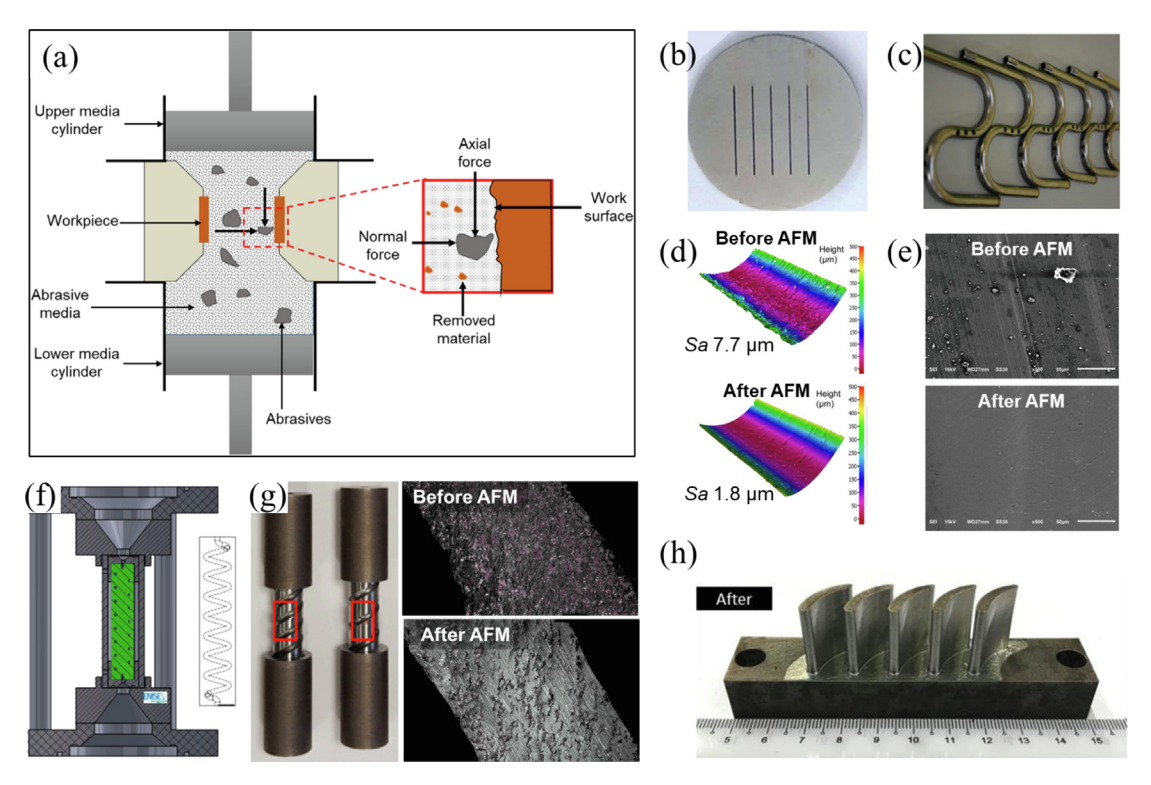


Fig. 5 (a) Schematic diagram and materials removal mechanism of AFM⁴⁰; (b) microslot⁴³ (c) bent pipes⁴⁵ that finished by AFM; (d) surface topographies⁴³ and (e) SEM images⁴⁵ before and after AFM; cooling channels (f) setup and (g) finishing results by AFM⁴⁶; (h) blade polished by AFM.⁴⁷

parameters (Fig. 5(c,e)). The experimental research found that the inlet pressure had a greater impact on the removal of the edge burrs of the cross hole, the fillet processing, and the inner surface roughness. Increasing the inlet pressure can effectively improve the finishing effect on the side hole wall. Finally, the internal surface quality of Ra 0.180 μ m in the opening was obtained. Kum⁴⁷ et al. polished multiple nozzle guide vanes at the same time by designing the fixture. The roughness of vanes was reduced from 13–15 μ m to less than 1 μ m under the condition of ensuring shape accuracy (Fig. 5(h)).

Currently, AFM is the most feasible solution for finishing parts with complex inner surface structures. Its flexible adaptability makes it widely used in various fields, including daily production processing and high-end precision areas. 19 After AFM, the inner wall can get a mirror finish. AFM can finish various types of workpieces, including long straight pipes, bent pipes, and multi-channel pipes. 42,45,46 Almost any channel that transports fluid can be finished by AFM to a certain extent. However, the surface roughness after AFM is highly dependent on the initial surface quality⁵. When the initial surface is poor, such as additive manufacturing parts, where the initial roughness is often higher than 10 µm, AFM can only reduce the roughness by one order of magnitude. To achieve submicron or even nanometer roughness, parts with better initial roughness are necessary. Moreover, AFM equipment is relatively complex, and a corresponding fixture should be designed for each workpiece, making the operation complicated and inefficient, which means that AFM is not suitable for small batch production.⁴⁰ The processing process of AFM mainly depends on the rheological characteristics of the abrasive (polymer medium), which makes controllability of the processing difficult. Uneven finishing and abrasive clogging often occur. These problems have prompted scholars to continuously develop new inner surface finishing technologies.

2.2.2. Abrasive jet polishing

Abrasive jet polishing (AJP) utilizes high-speed abrasive particles to impact the surface of the workpiece to achieve material removal. When processing the outer surface of the workpiece, the abrasive particles are ejected from the nozzle at high speed under pressure, and there is no direct contact between the nozzle and the processed surface; when processing the inner wall surface of the workpiece, it is usually necessary to design a pipeline to connect the high-pressure slurry outlet with the inlet of the workpiece channel. Generally, the media carrying the abrasive particles are air, water or other low-viscosity fluids, which can achieve high speeds at high pressures, whereas abrasive flow machining are unable to achieve high speeds due to the use of high-viscosity polymers. 48,49

Compared to AFM, AJP can achieve higher flow velocities due to the availability of low viscosity fluids and relies primarily on velocity impact for material removal. Cheung, et al. of developed a novel multi-jet polishing tool for precision polishing of internal surfaces. This method utilizes a rod-shaped nozzle with a row of linear holes along its side to probe the internal area of a 304 stainless steel cylinder. However, this method is only suitable for straight tubes with specific inner diameters. When the size decreases and the structure become more complex, the tool can no longer access the internal area effectively. Furumoto, et al. and of the cooling channel in an injection mould, where a solution containing free abrasive particles

was passed through the cooling channel by applying internal pressure to a hydraulic cylinder. The high velocity flow of free abrasive particles led to an increase in their kinetic energy, which increased the collision force with the inner surface, resulting in an improvement in the surface roughness. The better accessibility of low-viscosity fluids allows for the finishing of workpieces with smaller hole sizes.

Due to the stability of water, it is possible to add chemical reagents to the water or to utilize the physical effects associated with water to enhance the finishing efficiency and improve the quality of the internal surface. Deng, et al.⁵² proposed an abrasive flow polishing method based on the characteristics of self-excited oscillation pulses (Fig. 6(b)). The self-excited oscillation cavity is used to generate oscillation pulses from the abrasive flow, which effectively solves the problem of difficult finishing of slender pipes and the inner walls of micropores, reduce the roughness Ra of the inner wall of the stainless-steel pipe fittings from 480 nm to 50 nm. Nagalingam, et al. 53,54 presented a novel hydrodynamic cavitation abrasive finishing (HCAF) technique, and the feasibility for surface finishing of the method is analyzed (Fig. 6(c)). Various surfacefinishing conditions were employed to investigate material removal and additively manufactured AlSi10Mg internal channels were surface finished in isolated conditions of a) liquid impingement, b) absolute cavitation erosion, c) absolute abrasion, and d) cavitation assisted microparticle abrasion. The synergistic effects yielded 80% higher material removal and over 90% (*Ra*) higher surface-finish enhancement in HCAF conditions than those from pure cavitation and abrasion. AJP can also employ multiphase flow as the medium to carry abrasives to impact surfaces. Gu, et al.⁵⁵ proposed a novel approach to multi-phase jet (MPJ) polishing, utilizing a self-developed polisher that incorporates solid, liquid, and gas phases. After jet polishing, surface roughness (*Sa*) on the interior surface of grooves decreases from pristine 8.596 µm to 0.701 µm via MPJ polishing, and *Sa* reduces 96%, correspondingly (Fig. 6(e-i)).

Abrasive jet polishing with low-viscosity medium is suitable for various complex and micro-sized inner surfaces due to its characteristics of flexible materials removal. Compared with AFM, it has lower viscosity, avoids the risk of clogging. The relative low friction loss of the medium makes it more suitable for processing extremely small-diameter inner holes. It holds significant research value and promising application prospects in the field of precision finishing. But there are still some serious problems for its further application. Due to the high-speed movement of the fluid, when the slurry flows through the corner or the inner diameter changes step by step, the kinetic energy of the fluid is greatly lost, which is prone to uneven polishing. For a bent tube finishing, the velocity in the side with bigger radius of curvature is inevitably higher than the other side, which leads to uneven polishing as well.

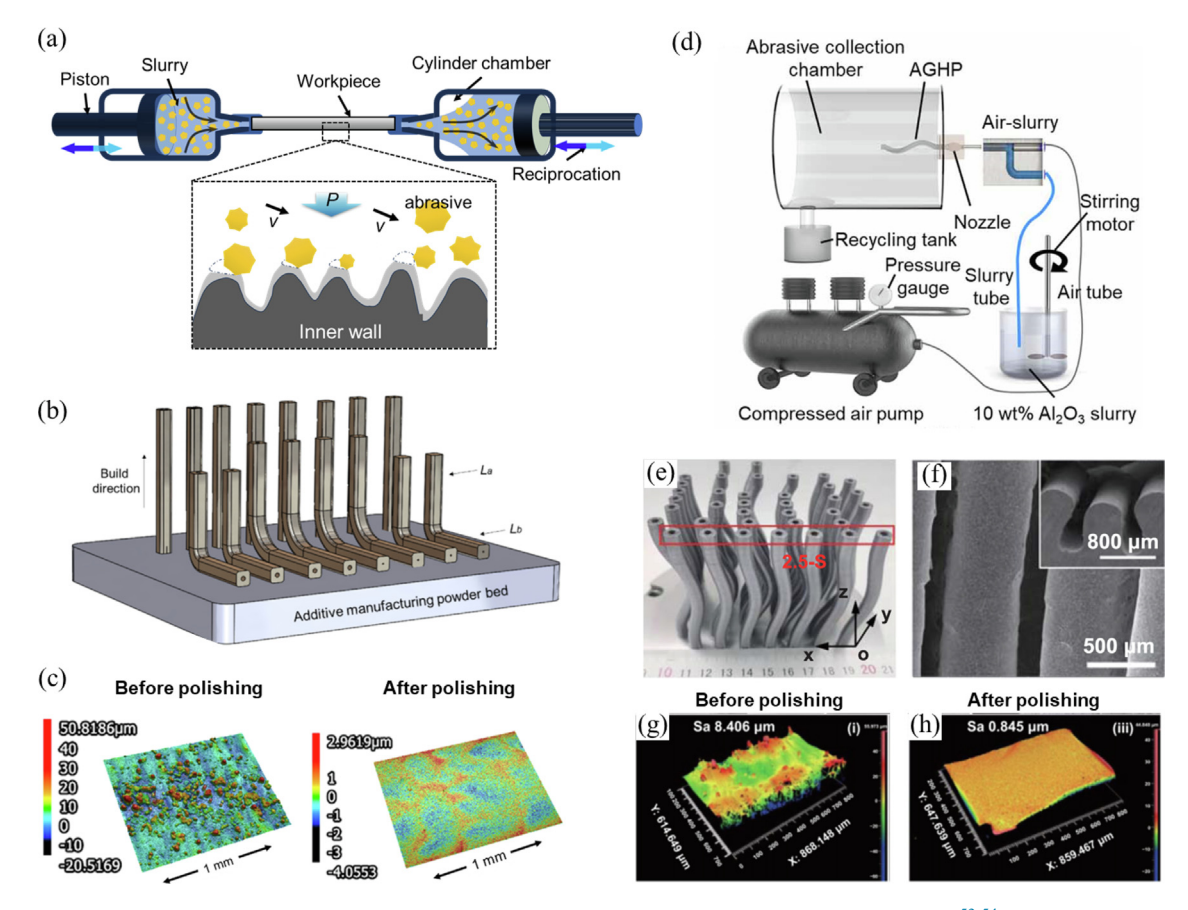


Fig. 6 (a) Schematic diagram of AJP; (b) prototype of linear and non-linear channels in rocket injector, ^{53,54} and (c) the internal surface before and after polishing; (d) equipment, (e) whole and (f) detailed view of workpiece, and the internal roughness (g) before and (h) after polished by multi-phase jet. ⁵⁵

2.2.3. Fluidized bed polishing

Fluidized Bed Polishing (FBP) is a relatively new surface polishing technology. Barletta et al. first proposed the FBP for workpiece processing in 2001. 56 In the FBP system, numerous abrasive particles are suspended in the moving fluid, and the interaction between the fluid and the abrasive particles makes the abrasive particles fluidized. Under the influence of fluid dynamic forces, fluidized abrasive particles are sprayed onto the workpiece at high velocities and precise impact angles, primarily targeting the protruding peaks and asperities on the surface to be machined. This process involves plowing and even cutting these asperities, thereby achieving the desired material removal rate and surface quality.⁵⁷ The basic fluidized bed apparatus is shown in Fig. 7(a). The main component of this device is the fluidized bed column, with a porous plate distributor at the bottom that ensures the fluid is supplied evenly throughout the entire column. The workpiece is positioned within the fluidized bed, either in a fixed or rotating state.

Building on the basic abrasive fluidized bed, Barletta et al. developed a hybrid processing technology that combines the FBP and abrasive jet machining, known as fluidized bed assisted abrasive jet machining (FB-AJM). The schematic diagram of the FB-AJM is shown in Fig. 7(c). Barletta et al. employed two interconnected fluidized beds to reciprocate fluidized alumina abrasives to both sides of the workpiece, while progressively decreasing the abrasive particle size, successfully reducing the average roughness of the inner surface of tubular workpieces made of SS 316L, with an inner diameter of 12 mm and a length of 200 mm, from Ra 1.5-4 µm to Ra 0.015 µm (Fig. 7(d)).⁵⁸ FB-AJM has also been applied to the precision finishing of inner surfaces of pipes with high length-todiameter ratios. After four processing cycles, the average surface roughness of a pipe made from Inconel 718 SPF, with a length of 100 mm and a diameter of 10 mm, was reduced from Ra 1.3–1.4 µm to Ra 0.11–0.14 µm, with the machined surface exhibiting minimal residual stress. 59 Additionally, for components with complex shapes, the fluidized bed system also demonstrated excellent machining performance. As shown in Fig. 7(e) and (f), FBP effectively smoothed and leveled the surfaces of holes and bosses on aluminum cast workpieces, and removed burrs from edges, demonstrating its reliability and flexibility.⁶⁰

As a no-pressure-copying finishing technique, FBP achieves material removal from the workpiece surface through fluidized abrasive particles, enabling the small-batch production of complex-shaped workpieces with good flexibility and processing efficiency. The combination of AJP with FBP further improves the abrasive supply system and facilitates the uniform distribution of abrasives on the inner surfaces of workpieces, achieving even material removal. Additionally, FBP supports the recycling of abrasives, thereby reducing environmental pollution and promoting ecological sustainability and production safety. However, the design and manufacturing of fluidized bed polishing systems are typically intricate, requiring precise control of fluid dynamics parameters, and involves high investment and maintenance costs. Moreover, FBP has certain limitations. While FBP is suitable for complex-shaped workpieces, traditional finishing methods may be more efficient and economical for simpler shapes.

2.3. Energy-field-based finishing

2.3.1. Magnetic abrasive finishing

Magnetic abrasive finishing, a precision finishing technique, was pioneered in 1938.⁶¹ The technology utilizes permanent magnets or electromagnets to create a magnetic field that could magnetize ferromagnetic particles with grinding ability. These particles align along the magnetic field lines, forming a magnetic abrasive brush with a certain rigidity. As the workpiece undergoes relative motion with magnetic abrasive particles, such as rotation, the magnetic abrasive brush, formed under the action of the magnetic field, performs micro-grinding, extrusion and collision on the surface of workpiece, so as to enhances surface quality and achieves the precise finishing of internal surfaces.⁶²

In the realm of inner surface processing, MAF technology can be classified into two distinct types based on the positioning of the magnetic poles: internal magnetic pole type and

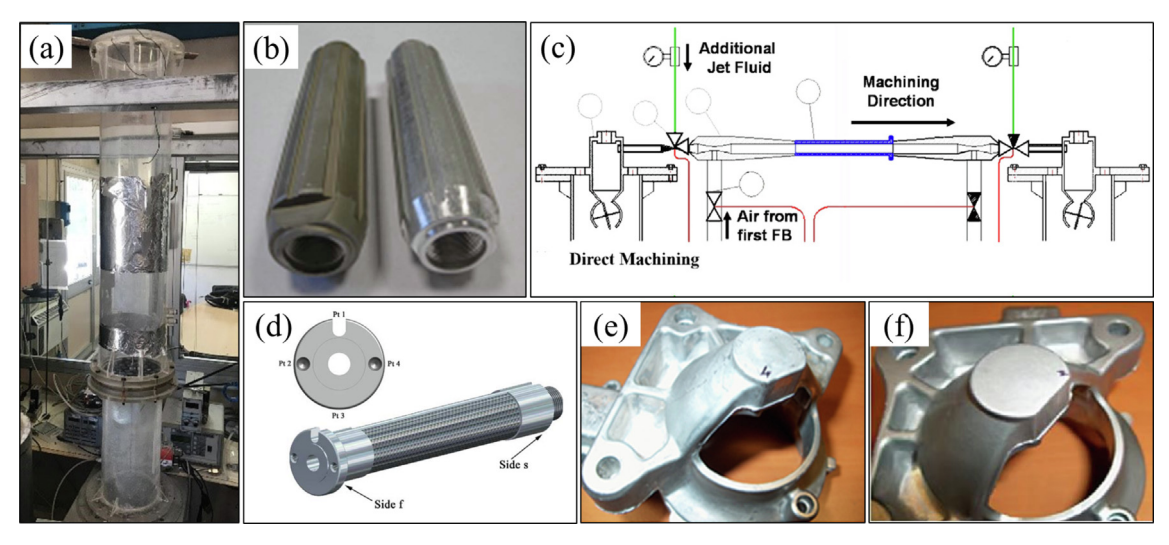


Fig. 7 (a) Basic fluidized bed apparatus; (b) tubular parts with made of AA 2024 O alloy⁵⁶; (c) schematic diagram of FB-AJM; (d) SS316 channel polished by FBP; aluminum casting parts with complex structure (e) before and (f) after polished by FBP. ^{58–60}

external magnetic pole type, 63 as illustrated in Fig. 8. The primary difference between these two types lies in the placement of the magnetic poles and abrasives. In the internal magnetic pole finishing, both the abrasive and the magnetic pole are situated inside the channel. Conversely, in the external magnetic pole finishing, the abrasive is placed inside the channel while the magnetic pole is positioned on the outer surface of channels. Compared to the external magnetic pole type MAF, the internal magnetic pole type MAF has certain limitations due to the size and structure of the magnetic pole. For instance, Verma, et al.⁶⁴ proposed a novel finishing tool based on an internal magnetic pole. By positioning two permanent magnets with similar poles facing each other, a high magnetic flux density is generated in the circumferential region between the magnets. Through the optimization of processing parameters, the internal surface roughness of a \varnothing 24 mm \times \varnothing 20.1 mm \times 60 m m stainless steel (SS304) pipe was successfully reduced to 56 nm. However, this method is more similar to machining processes that require finishing tools to enter the inside of channels, such as honing. It is suitable for finishing largediameter straight pipes but has limited accessibility for curved pipes or small-diameter pipes. Therefore, the following section will focus on the external magnetic pole type MAF.

Currently, the external magnetic pole type MAF have been successfully applied to a variety of internal surfaces with small apertures. Yamaguchi, et al. 65 utilizes diamond abrasives to finishing the inner surface of a ceramic tube with a dimension of \emptyset 20 mm × \emptyset 15 mm × 150 mm (Fig. 9(a)). This process successfully reduced the surface roughness of the ceramic inner

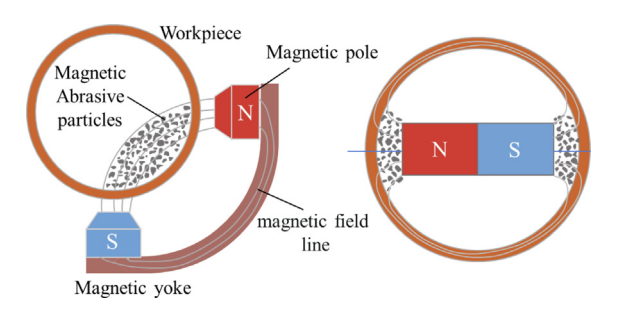


Fig. 8 Position of magnetic poles: (a) external magnetic pole type, (b) internal magnetic pole. ⁶¹

tube from 3 µm to 0.02 µm, enhancing the shape accuracy and surface quality while reducing residual stress. Based on the conventional MAF technique, the multi-energy fieldassisted MAF technique has been developed, including vibration assisted magnetic abrasive finishing (VFAM), ultrasonicassisted magnetic abrasive finishing (UAMAF), and chemically assisted magnetic abrasive finishing (CMAF). Guo, et al.66 introduced an auxiliary magnetic pole in the gap between the outer and inner tubes of an Inconel double-layer tube manufactured via the SLM process (Fig. 9(b)). By combining workpiece rotation with linear magnet vibration, they achieved the finishing of the gap. The surface roughness of the inner and outer surfaces of the inner tube was reduced from 7 um to less than 1 um, eliminating surface corrugations and scratches, resulting in a non-damaging machined surface, as depicted in Fig. 9(c). Yun, et al.⁶⁷ designed an ultrasonicassisted magnetic abrasive finishing device that introduces ultrasonic vibration to the magnetic pole, altering the path of the magnetic grinding brush. Compared to conventional MAF, the approach significantly improves the material removal rate and reduces non-uniform texture on the inner surface. The surface roughness was decreased from 1.1 µm to 0.03 µm, achieving efficient and precise finishing of the inner surface. Singh, et al. 68 proposed a chemically assisted magnetic abrasive finishing technique for the inner surface of Inconel 625 pipes. By treating the internal surface with a ferric chloride and ethanol chemical solution, weakened the surface molecular bonds, effectively eliminating irregular and diffused surface features, and improving the roundness of the tube.

With the continuous advancement of MAF technology, its applications have expanded to the finishing of inner surfaces of high aspect ratio capillary tubes and complex curved pipes. Yamaguchi, et al. ⁶⁹ designed a single tip MAF device specifically for finishing the inner surfaces of stainless-steel capillaries with inner diameters less than 1 mm, and they successfully reduced the inner surface roughness of capillaries with dimensions \emptyset 0.5 mm× \emptyset 0.4 mm × 60 mm from 2.05 µm Rz to 0.15 µm Rz (Fig. 9(d–f)). Building on this, Yamaguchi and colleagues utilized selective heat treatment to create a metastable magnetic tool capable of producing alternating magnetic and non-magnetic regions. Consequently, they developed a multiple pole-tip system and high-speed multiple pole-tip finishing equipment, enabling simultaneous finishing of multiple areas

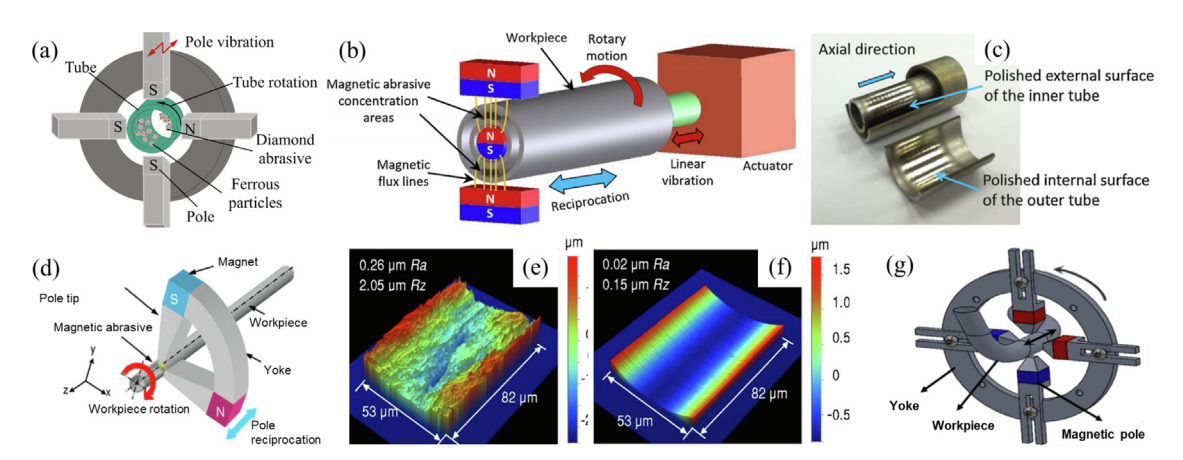


Fig. 9 (a) MAF set-up for a ceramic tube⁶⁵; (b) schematic diagram and (c) polished surface of double-layer tube⁶⁶; (d) schematic diagram and (e) before and (f) after polished surface of capillary tube⁶⁹; (g) schematic diagram of MAF for bent tube.⁷⁰

within capillary tubes, $^{70-73}$ thus significantly enhancing finishing efficiency. This high-speed equipment can produce a finished surface 50.8 mm long in just 10 min, with a roughness of approximately 0.1 μ m Rz. Nteziyaremye, et al. 74 added magnetic abrasive particles to both the inner and outer surfaces of $\varnothing 1.27$ mm $\times \varnothing 1.14$ mm $\times 100$ mm stainless steel tubes. Under the action of the external magnetic pole, the inner surface and the outer surface of the needle were simultaneously polished by rotating the tube, reducing the roughness of both surfaces from Sa 0.4–0.5 μ m to 0.01 μ m within 5 min, thereby significantly reducing processing time.

For ultra-long capillaries, Deng, et al. 75 prepared the magnetic abrasive particles with different sizes to finish the inner surface of ultra-fine and ultra-long Ni-Ti allov pipes $(\emptyset 1.36 \text{ mm} \times \emptyset 1.24 \text{ mm} \times 1200 \text{ mm})$. The process successfully removed defects such as wrinkles and cracks, reducing the surface roughness from Ra 0.75 µm to 0.08 µm. As for curved tubes, Yamaguchi, et al. 70 achieved local enhancement of the magnetic field by offsetting the pole rotation axis from the curved shaft. This technology was applied to the surface processing of SUS304 stainless steel curved tubes with inner dimensions of $\varnothing 10 \text{ mm} \times \varnothing 8 \text{ mm} \times 64.4 \text{ mm}$. The surface roughness of the curved tube surface was reduced to 0.1 µm Ra. For irregular bend structures, Yu, et al. 76 utilized the centerline reconstruction method to determine the irregular geometric centerline of the space bend and optimized the finishing path accordingly. They successfully reduced the surface roughness of \(\infty 26 \text{ mm} \times \(\infty 22 \text{ mm} \times 80 \text{ mm} \text{ titanium} \) alloy curved tubes to 0.11 µm, as shown in Fig. 9(g).

As a magnetic field-assisted finishing technology, MAF technology finish the inner surfaces of pipes using a magnetic abrasive brush formed by ferromagnetic particles, which makes it have several advantages, including high precision, self-sharpening capabilities, low residual stress, and excellent profile adaptability. Additionally, the processing equipment for MAF is typically simple, and the processing cost is relatively low. Consequently, MAF is widely utilized for finishing various types of straight pipes, curved pipes, and even capillary tubes. However, the application of MAF technology is limited by the constraints of the magnetic field. It is primarily suited for processing tubes with thin walls and is not effective for structures with thick walls, such as conformal cooling channels. Furthermore, when applied to the finishing of nonrotationally symmetric parts, MAF can lead to uneven material removal.

2.3.2. Electrochemical polishing

In the 1980 s, electrochemical polishing (ECP) began to be applied to the internal surface polishing of stainless-steel tubes. The ECP involves using the workpiece as the anode and an auxiliary electrode, typically made of conductive materials such as platinum or graphite, as the cathode. Working medium can be transmitted through a specific electrolyte between the electrodes, which can be acidic, neutral, or alkaline. Electrochemical parameters such as current, voltage, temperature, electrolyte concentration, and processing time significantly influence the efficiency and quality of electrochemical machining of metals. By applying voltage and fine-tuning these electrochemical parameters, oxidizing reactions occur on the workpiece surface, leading to its dissolution and materials removal. Due to the tip effect, small protrusions on the surface

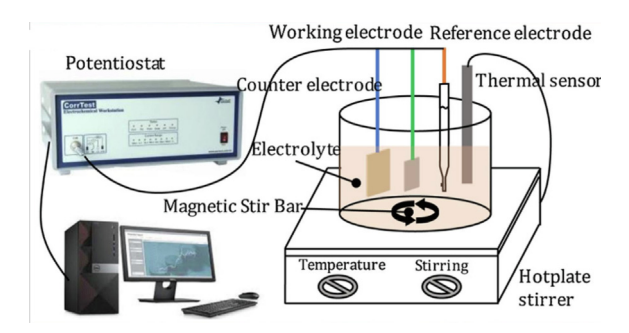


Fig. 10 Experimental set up for EP process. 19

with high charge density undergo electrolysis at a faster rate than areas with relatively lower charge density. This results in the preferential dissolution of these protrusions, gradually leading to a smoother metal surface and finishing, achieving the finishing of the surface.¹⁹ The experimental equipment of ECP process is shown in Fig. 10.

The underlying materials removal process in ECP was not fully revealed yet. There are several widely accepted theories explaining the electropolishing mechanism, including viscous film theory, ⁷⁷ passivation theory, ⁷⁸ double-layer film theory and so on. According to the viscous film theory proposed by Jacquet, the dissolution of rougher surfaces results in the formation of an uneven mucous membranes. The film is thicker in the valleys, exhibiting high resistance and low potential distribution, which leads to slower dissolution rates. Conversely, at the peak positions, the membranes are thinner, resulting in a greater material removal. Building on the viscous film theory, Hoar et al. proposed the passivation film theory, which posits that a thin passivation film forms on the anode surface during ECP. Due to the difference in resistance and potential distribution, the oxide film at the peaks is more prone to detachment, leading to faster dissolution at these peaks. As polishing progresses, the disparities between the peaks and valleys diminish. the thickness of the oxide film stabilizes, and the surface becomes smooth and flat. The double-layer film theory integrates the preceding theories, suggesting that two layers of film form on the electrode surface during ECP: an inner passivation film and an outer viscous liquid film. The inner passivation film provides initial protection to the metal surface, while the outer viscous liquid film regulates the flow of the electrolyte and ion transport. The interplay between these two layers determines the dissolution behavior of the surface metal, thereby achieving the desired polishing effect.

As a non-contact process, ECP employs electrolytes and electric fields to dissolve and polish metal surfaces, thereby overcoming the limitations inherent in traditional mechanical polishing tools. Ro-86 This allows for the polishing of various pipeline structures with ease. Fayazfar, et al. developed an anhydrous, alcohol-based electropolishing solution to achieve efficient finishing of the internal surfaces of Ti-6Al-4 V parts manufactured by LPBF. Through precise control of ECP parameters, their research demonstrated significant improvements in the inner surface finishing of straight pipes of different shapes, including round, square, and U-shaped pipes, achieving a maximum surface roughness improvement of 77% (Fig. 11(a)). Similarly, Ali et al. successfully polished the internal surfaces of Inconel 625 parts using ECP. They reported reductions in Sz for square, circular, flat square bent,

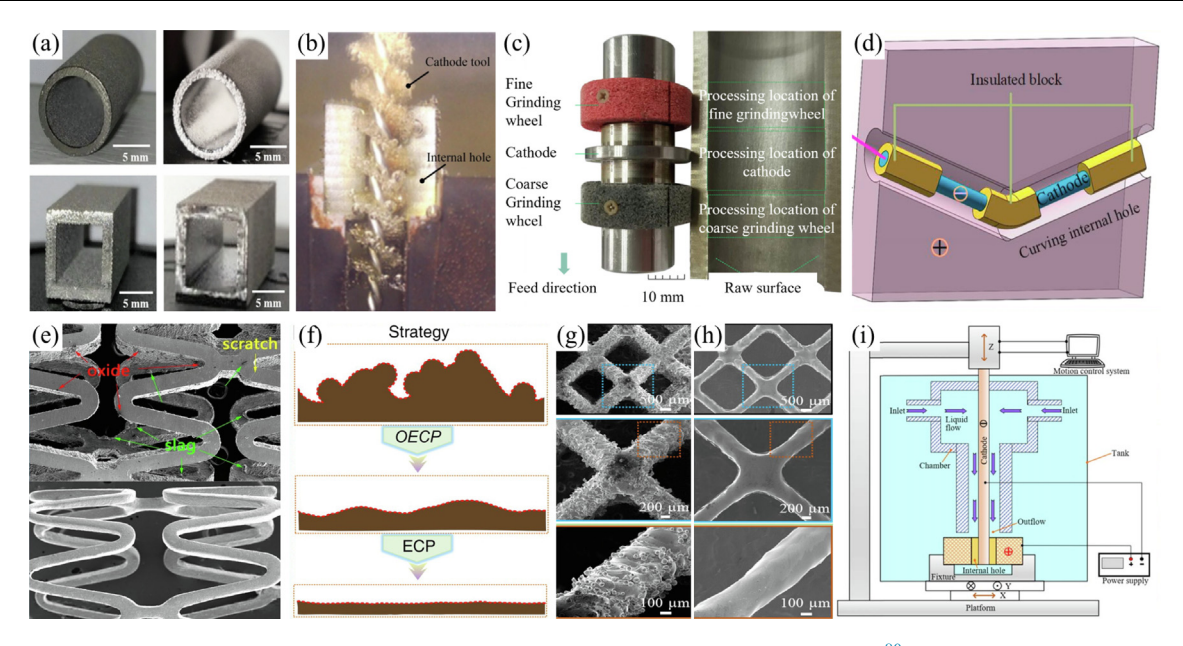


Fig. 11 (a) Optical images of as-built (left column) and electropolished (right column) samples⁸⁰; (b) ECMP process for the internal hole⁸²; (c) Tool component and respective finishing areas⁸³; (d) Schematic diagram of flexible cathode tool; (e) Ni-Ti cardiovascular stent before and after ECP⁸⁴; (f) Strategy for smoothening of as-printed side surface, a combination of OECP and ECP; (g) Morphology of lattice surface before and (h) after OECP for 40 min⁸⁵; (i) Schematic diagram of closed ECP for coaxial electrolyte flushing.⁸⁶

and curved square bent tubes by 68%, 34%, 84%, and 74%, respectively.

The integration of electrochemical and mechanical polishing techniques offers a potentially cost-effective solution for internal surface finishing. Zhao, et al.82 developed a cathode tool that combines a metal electrode with a non-conductive flexible abrasive (Fig. 11(b), enabling an electrochemical mechanical polishing (ECMP) process. During the electrochemical reaction on the inner surface, the cathode tool moves, causing the flexible abrasive to mechanically scratch the surface. This dual-action process successfully reduced the surface roughness Sa of a straight hole in SLM-manufactured 304 stainless steel pipes from 14.151 µm to 3.880 µm. Similarly, An, et al.83 introduced an electrochemical mechanical combined polishing process for additively manufactured parts with internal channels. Their tool comprises a coarse grinding wheel, fine grinding wheels, and a cathode (Fig. 11(c). In the EMCP process, coarse grinding wheels initially remove adhesive powders, followed by electrochemical polishing with high current density to dissolve micro-bumps. This method effectively polished small diameter straight and curved grooves $(\emptyset 5 \text{ mm and } \emptyset 9 \text{ mm})$, reducing surface roughness (Sa) from 15.92 μm and 18.18 μm to 5.06 μm and 6.02 μm, respectively.

ECP is particularly well-suited for surfaces that are challenging to access with traditional finishing methods, such as curved pipes, cardiovascular stents, open porous structures, high aspect ratio holes, and microscopic channels. For curved tubes, specially designed electrodes are employed to mitigate uneven polishing caused by electrode shape, spacing, and other factors. Kim, et al.⁸⁷ solved the polishing of L-shaped bend tubes made of STS 316L stainless steel by using L-shaped cathode formed by placing two copper cathodes inside the tube. Zhao, et al.⁸⁸ developed a flexible cathode tool to polish the curved inner holes of 304 stainless steel produced through additive manufacturing (Fig. 11(d)). By moving the flexible cathode, equipped with an insulating block, along the inner

surface of the curved hole, adhesive powder was effectively removed, and the surface roughness (Sa) was reduced from 15.522 µm to 8.102 µm. For cardiovascular stents, Wang, et al. ⁸⁴ compared the polishing effects of three electrolytic polishing solutions—acid-acid, acid-alcohol, and alcohol-salt—on nitinol cardiovascular stents. The experimental results indicated that the sodium chloride-ethylene glycol ECP solution obtained the best results, achieving a minimum surface roughness (Ra) of 1.84 nm (Fig. 11(e)).

As for the research of porous structures, Pyka, et al. 89 successfully removed metal powder particles from the surface of Ti6Al4V open porous structures produced by selective laser melting (SLM) using a combination of chemical etching and ECP, thereby reducing surface roughness. However, conventional ECP tends to suffer from non-selective and nonuniform removal when polishing porous structures, limiting surface finish quality. To address these challenges, scholars proposed overpotential polishing technology. Gomez-Gallegos, et al.⁹⁰ demonstrated a close relationship between surface finish and overpotential during electrochemical machining (ECM). Chang, et al.⁸⁵ proposed an overpotential electrochemical polishing (OECP) strategy (Fig. 11(f)), which involves achieving highly selective removal of adhesive particles by selecting a potential slightly higher than the current plateau region (overpotential). Further smoothing is then accomplished through conventional ECP. The combination successfully reduced the surface roughness of SLM-prepared 316L stainless steel micro-lattices from approximately 8 µm (Fig. 11(g)) to 0.18 μm (Fig. 11(h)). In addition to overpotential polishing, a closed electrochemical polishing process using coaxial electrolyte flushing is employed for the uniform materials removal of the inner surfaces of high aspect ratio micropores.

ECP facilitates the removal of metal surface material through an electrochemical reaction, thereby circumventing the limitations of traditional polishing tools and the corre-

sponding mechanical property. This process enables efficient. high-quality finishing of various internal surface structures, including complex pipes, cavities, small channels, and high aspect ratio holes. Moreover, the longevity of ECP tools typically exceeds that of traditional mechanical tools, resulting in relatively low production costs. 86 In recent years, plasma electrolytic polishing (PEP) has developed rapidly, becoming a promising solution for complex structures, as it requires no shaped tools. However, ECP is highly sensitive to processing parameters such as voltage, current, and temperature. When polishing complex structures like porous materials, uneven polishing often occurs, leading to localized over- or undercorrosion, which subsequently compromises the original shape accuracy. Additionally, ECP is generally applicable only to conductive metal materials, making it unsuitable for nonconductive substrates such as ceramic or quartz tubes.

2.3.3. Multi-filed assisted finishing

As internal structures used in advanced industries become increasingly complex, finishing methods based on a single energy field are inadequate to meet the demands for surface quality, processing efficiency, and controllability of high-performance components. By analyzing the structural constraints of parts processing and leveraging the advantages of corresponding energy fields, mutual promotion between different energy fields can be achieved. Finishing methods based on multiple fields can accelerate material removal efficiency, enhance the controllability of the finishing process, and improve surface quality.

For example, magnetic fields can be used to envelop abrasive particles, improving their controllability, or to modify

the abrasive flow conditions, enhancing the overall controllability of finishing. Guo, et al. 91 proposed a new magneticassisted chemical abrasive flow polishing (MCAFP) method using a ferromagnetic blockage placed inside a tube to finish the internal surfaces of slender tubes with varying diameters (Fig. 12(a)). The results indicate that the specially designed ferromagnetic blockage effectively adjusts flow velocity and pressure, thus controlling local material removal. A uniform internal surface (Sa < 40 nm) was achieved when finishing a puncture needle with diameters ranging from 0.3 to 0.7 mm (initial Sa 600-1200 nm). Chemical action can soften the surface material of the workpiece, thereby improving the material removal efficiency of mechanical and other actions. Guo, et al. 92 proposed a new magnetic enhanced chemical mechanical polishing method for quartz glass slender holes (Fig. 12 (c)). This method achieves high-efficiency and high-quality polishing, significantly reducing the surface roughness Sa of slender holes from 0.3 µm to 77 nm, with a material removal rate of 141 µm/h. The results show that a synergistic effect is formed between multiple fields. Under the influence of the magnetic field, the contact pressure between cerium oxide particles and the quartz surface is improved, promoting material removal through a more adequate chemical reaction.

Mechanical action can be used to remove the oxide film generated during electrochemical polishing, thereby increasing the material removal rate of electrochemical polishing. Zhao, et al. 93 created a uniform and efficient flow field through coaxial electrolyte flushing, which promoted the discharge of electrolytic products. This method successfully removed partially melted powder adhering to the inner surface of additively manufactured parts, reducing the surface roughness (*Ra*) from

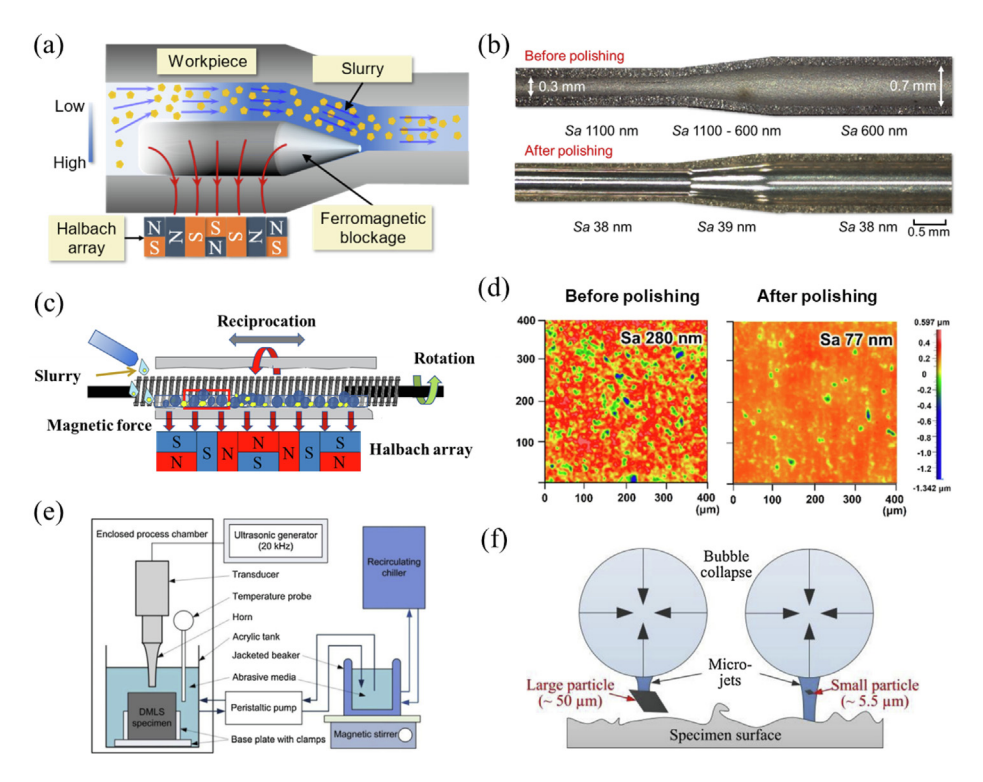


Fig. 12 (a) Principle of magnetic-assisted chemical abrasive flow polishing and (b) the puncture needle before and after polishing ⁹¹; (c) polishing mechanism of MCMP and (d) the polishing results of quartz⁹²; (e)the schematic diagram and (f)the micro-jet interaction with surface of UCAF. ^{93,94}.

 $15.620~\mu m$ to $3.494~\mu m$ and the peak-to-valley height from $78.402~\mu m$ to $19.272~\mu m$.

Ultrasonics is a commonly used energy field to enhance the finishing process. Ultrasonic-assisted polishing can utilize the micro-impacts generated by ultrasonic vibrations to enhance the contact frequency between abrasives and the workpiece, as well as improve the fluidity of the polishing solution. This leads to increased polishing efficiency and improved surface quality. Ultrasonic action, in conjunction with fluid, can also induce cavitation effects. The transient high temperatures and pressure impacts generated by cavitation bubbles enhance the kinetic energy of abrasive particles as they jet the workpiece, resulting in effective material removal. Tan, et al.94 designed an ultrasonic cavitation abrasive finishing (UCAF) device and conducted polishing experiments on the inner hole of an additively manufactured cubic workpiece with an inner diameter of 3 mm as shown in Fig. 12(e). The experimental device uses an ultrasonic device to generate cavitation effect and cooperates with abrasive impact to remove material from the workpiece. The author explored the influence of different process parameters such as abrasive particle size, abrasive concentration, ultrasonic amplitude and polishing gap on the Ra value and Rz value, and used the optimal parameters to reduce the average surface roughness Ra of the inner hole with an inner diameter of 3 mm from 6.5 µm to 3.8 µm.

By integrating the physical fields and leveraging the advantages of various energy fields, multi-field assisted polishing technology can effectively overcome the limitations of traditional polishing methods. Through precise control of magnetic, electric, and ultrasonic fields, this technology can achieve efficient polishing of workpieces made from different materials, with varying shapes and sizes, significantly enhancing the final surface quality. Although multi-field assisted polishing is rapidly developing, it still inherits the limitations of each individual field. Ensuring synergistic interactions between the energy fields is essential. However, the numerous parameters influencing multi-field assisted polishing present chal-

lenges, and the coupling mechanisms between these fields have not been sufficiently explored. The synergistic enhancement mechanisms among multiple fields require further investigation.

3. Internal surface roughness measurement technology

Internal surface roughness measurement involves obtaining two-dimensional or three-dimensional shape information of a part's inner surface. By analyzing low-frequency data, the geometric accuracy of the inner surface and the location of defects can be assessed. High-frequency information analysis provides details on the internal surface roughness. Internal surface measurement technologies generally include contact and noncontact methods, as well as optical and non-optical techniques. This chapter is divided into tool-probing measurement technologies and non-probing measurement technologies based on whether a tool head is used.

3.1. Tool-probing measurement

3.1.1. Stylus-probing method

Contact measurement is the earliest method employed for assessing the surface roughness of machined parts, with its research history dating back to 1927. In 1936, E.J. Abbott developed the first surface roughness profilometer suitable for use in production environments⁹⁵. This innovation paved the way for rapid advancements in stylus-probing method, epitomized by the roughness profiler⁹⁶.

The principle of stylus-probing method is illustrated in Fig. 13(a). As the stylus lightly traces the surface of the work-piece, it moves vertically in response to the peaks and valleys of the surface profile. ^{97–103} This displacement signal is converted into an electrical signal by a sensor, then filtered and amplified. The processed signal is subsequently output by recording instruments as roughness data (*Ra*, *Rt*, *Rmax*) or

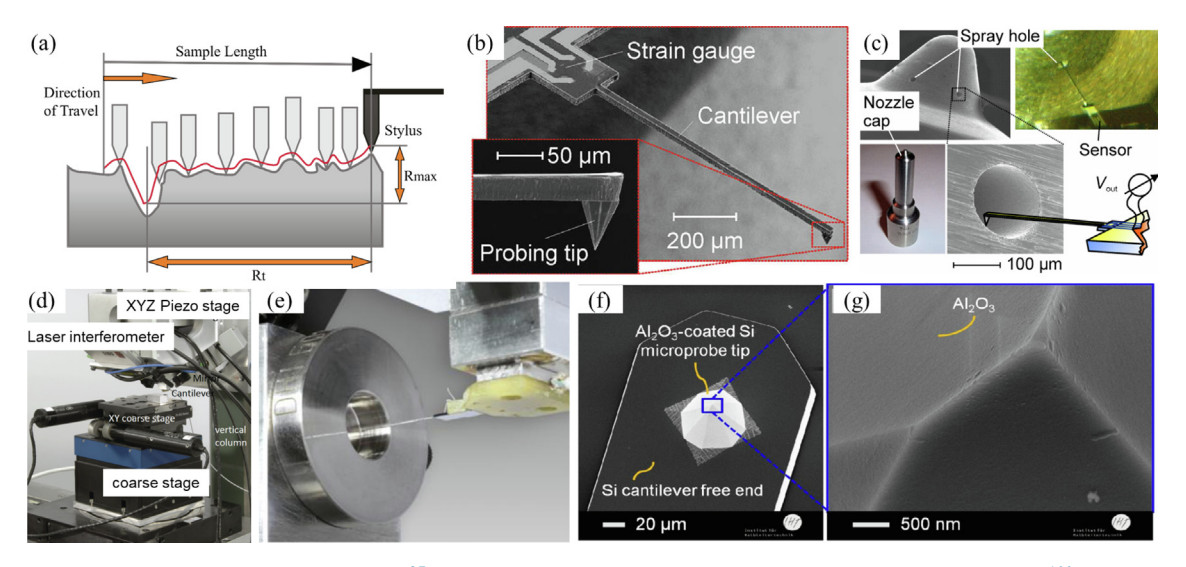


Fig. 13 (a) Principle of stylus-probing method⁹⁷, (b) Scanning electron micrograph of silicon cantilever sensor 100 ; (c) Piezoresistive sensor accessing a fuel injector nozzle spray hole 101 ; (d) Profile scanner set-up; (e) Microprobe in front of a nozzle with 800 μ m diameter 102 ; (f) Silicon microprobe tip on the bottom surface of piezoresistive microcantilever sensor after (g) thin Al_2O_3 film coating by ALD. 103

profile curves related to the measured surface. The measurement process is not only quick and convenient but also highly accurate and cost-effective, making it widely applicable for measuring various surfaces such as flat, curved, internal bores, and narrow grooves.

For larger diameter internal surfaces, sufficient working space allows measuring instruments to directly insert the probe into the area to conduct roughness measurements. In contrast, for measuring the morphology of the internal surfaces of slender tubes, stylus-probing equipment typically achieves roughness measurement of deep holes by extending the measuring rod. Zhang, et al. 97 designed a measuring device capable of automatically detecting surface roughness at multiple points within deep holes. This device utilizes an extended measuring rod in conjunction with rotational and linear motions of the components, enabling multi-point automatic detection along multiple busbars of internal holes with diameters ranging from 16 to 25 mm and lengths from 120 to 180 mm. The detectable Ra value range is 0.01 to 1.6 μ m.

As the diameters of machined internal holes continue to decrease, especially with the advent of high aspect ratio micro-holes such as those in diesel injector nozzles, new demands have emerged for contact-based roughness measurement techniques. Lebrasseur, et al. 98 proposed a system for measuring the internal contours of high aspect ratio microstructures. This system utilizes a silicon probe with an integrated piezoresistive force sensor, measuring 1 mm in length and having a cross-sectional area of 20 μ m \times 20 μ m, to assess the roughness of micro-holes with a radius as small as 40 µm and 200 µm in depth. Subsequently, Peiner, et al. ^{20,26,99–101} developed a mass-producible, piezoresistive silicon micro-cantilever sensor for the non-destructive, rapid detection in high aspect ratio deep and narrow micro-holes, such as those in diesel injector nozzles. These silicon microcantilevers range from 1 to 5 mm in length, 30 to 200 µm in width, and 25 to 50 µm in thickness, with probe tip heights between 25 and 50 µm and contact radius smaller than 100 nm. This significantly extends the measurement depth of the cantilever probe with the minimum measurable diameter to 75 µm. Additionally, the sensor still maintained micronlevel lateral resolution and 10 nm vertical resolution at higher scanning speeds ($> 200 \mu m/s$), thereby enhancing the precision and efficiency of deep micro-hole measurements. 20

Based on piezoresistive silicon cantilever sensors, Xu, et al. 102 developed a profile scanner that enables traceable roughness and profile measurements of high aspect ratio structures with diameters down to 50 µm. This device inherits the high-resolution advantages of the aforementioned cantilever probes, and three different specifications of micro-probes were employed to achieve roughness measurements of micro-holes with varying diameters and depths. Furthermore, by bonding two 5 mm long cantilevers together, a 7.5 mm long cantilever was created, allowing roughness measurement of the inner surface of a small sonic nozzle with a throat diameter of 800 µm and a measurement depth of no less than 5.6 mm for the first time. The measurement results were consistent with those obtained using standard stylus roughness measuring instruments, confirming the metrological capability of the contour scanner. 103 To minimize tip wear and enhance scanning speed, Wasisto, et al. 104 employed atomic layer deposition to coat the tip of the cantilever probe with Al₂O₃. Comprehensive wear tests were conducted on probes with the coating at a transverse

scanning speed of 15 mm/s and a detection force ranging from 60 to 100 μ N, demonstrating the efficacy of the Al₂O₃ coating. To further reduce tip wear, Brand, et al. ¹⁰⁵ introduced a low-wear spherical diamond tip with a radius of 2 μ m, replacing the original integrated silicon tip. Additionally, they developed a compact microprobe device with an integrated feed unit that has been successfully employed to measure the surface roughness of critical flow Venturi nozzles and diesel injection nozzles at high speed. Through the development of a theoretical dynamics model and the conduction of tip-flight tests on rapidly varying surfaces, Xu, et al. ¹⁰⁶ demonstrated that the microprobe equipped with an integrated silicon tip possesses the capability to accurately track surface topography during high-speed scanning.

As a contact measurement technique, the stylus-probing method serves as the foundation for both national and international standards due to its convenient application and high measurement accuracy. It has become the most widely used and developed method for measuring surface roughness. This method also offers additional advantages, such as a large measuring range and minimal environmental requirements.

However, it has some drawbacks as well, including the limited scanning speed of the probe, rapid wear of the probe tip, measurement error caused by probe tip vibration, excessive detection force to scratch the surface of the workpiece and so on. Furthermore, the measurement of deep micro-holes presents challenges due to the confined working space, which imposes stringent requirements on the size and stiffness of the probe and rod, as well as the ratio of length to diameter.

3.1.2. Optical interference method

Optical interference technology involves the combination of a light beam reflected, refracted, or diffracted by the object under measurement and another beam of light emitted by the reference mirror surface, resulting in interference fringes. Light-sensitive detection components like CCD cameras convert the fringe intensity into an electrical signal, which is then used for data processing to obtain the micro-topography information of the measured object's surface. Due to the rapid development of computer technology, CCD imaging technology, and digital image processing technology, automated and efficient processing of interference fringes has become feasible. Optical interference has become one of the primary methods for high-precision measurement of part surface morphology. Interference fringes serve as carriers of surface contour information. Valuable information contained in the fringes can be obtained through analysis of the interference fringes. 107

Optical interference technology is commonly used for micro-measurements through two main methods: phase-shift interference measurement technology and white-light interference measurement technology. Phase-shift interference measurement technology typically utilizes lasers as light sources, which offer long coherence lengths enabling the acquisition of interference fringes over a wide range of optical path differences. 109-112 Li 109 developed a polarizing phase-shift interference measurement system based on the principle of phase-shift interference microscopy and designed an engineered measurement head to construct a measurement system for the micro-surface morphology of inner walls of tubular optical components. This system achieved microscopic surface morphology detection of the inner walls of metal pipes with an

inner diameter of 50 mm and laser gain tubes with a diameter of 42 mm, with a vertical resolution less than 2 nm, roughness measurement error about 1.5 nm, and measurement repeatability better than 0.1 nm. The system obtained roughness and defect information for surfaces within a depth range of 0–80 mm. However, due to the periodic nature of phase, phase-shift interference technology can only measure surface height through phase analysis within a sub-wavelength longitudinal measurement range, limiting its ability to accurately measure surface information with large contour fluctuations (Fig. 14(b)).

To achieve a larger measurement range, phase-shift interference technology has been developed into white-light interference technology. White-light interference technology is also known as low-coherence interference technology. In white-light interference, all colors of light within the light source's spectral range can participate in interference and their interference intensity distributions are superimposed to form an interference image. The effective range of white-light interference fringes is proportional to the coherence length of the light source and inversely proportional to the spectral width of the light source. However, when using a white-light source with a very wide spectral range, interference fringes are only distributed near the length of the reference arm. To address this, Gao, et al. 110 developed an optical path model based on monochromatic phase-shifting interference technology and utilized a conical mirror to measure the inner surface of a smooth cylinder. The theoretical deduction was used to separate measurement system errors, such as conical mirror surface shape errors and alignment errors. Nevertheless, the measurement range of a single wavelength is limited and not suitable for measuring inner surfaces with microstructures and high roughness.

White-light scanning interferometry has a limitless theoretical measurement range, but practical limitations arise from the scanner's working range, typically achieving millimeterlevel range. However, it can still measure the threedimensional contours of rough or even discontinuous surfaces. Dong, et al. 111 developed a specialized structure for an innersurface white-light interferometry instrument to measure the micro-structural surface morphology of a 90 mm diameter part. The inner surface was observed by rotating the microscopic imaging path, achieving nanometer-level roughness measurement accuracy with an average deviation of less than 10 nm. Albertazzi¹¹² designed a white-light interferometer for measuring internal cylindrical or quasi-cylindrical parts. They conducted roughness measurements on a standard ring with a diameter range of 14-26 mm (Fig. 14(c)). A high-precision 45degree conical reflection mirror was utilized to guide the collimated light radially toward the test surface, and the image was distorted by the mirror, forming an image on the sensor plane of the digital camera. A mapping algorithm was used to reconstruct the cylindrical geometry from the distorted image, making it possible to measure the inner surface in true cylindrical coordinate.

In summary, optical interference technology is a non-contact measurement technique that has significant developmental significance in achieving surface measurements of workpieces without causing any damage. Its advantages include high precision, high resolution, and full-field measurement, making it suitable for measuring micro and nanostructures. It can also use data to measure different frequency bands simultaneously for processing algorithms. Consequently, it has become widely used in measuring precision inner wall parts, thus promoting the development of micronano manufacturing. However, the measurement system is

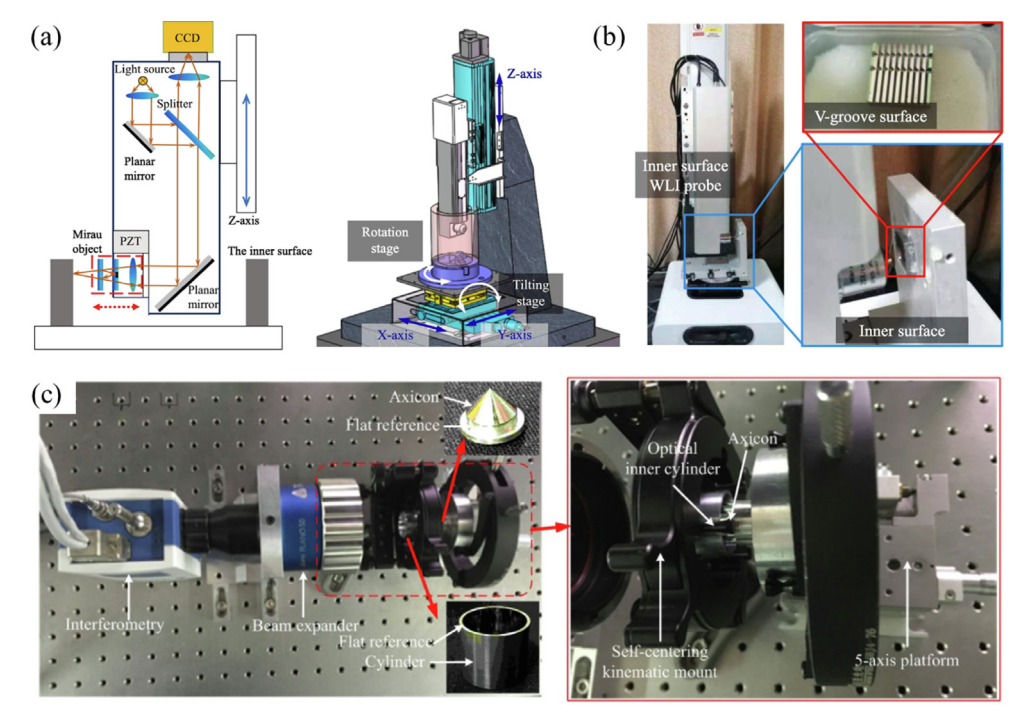


Fig. 14 (a) Diagram of designed inner surface WLI probe and (b) design model of inner surface WLI measurement system. (c) Experimental setup and Partial enlarged detail. (112)

prone to external environmental interference, leading to shaking interference fringes, making it unsuitable for industrial onsite measurements. Therefore, the current trend is to establish a robust hardware system to improve the measurement system's stability, use step compensation algorithms to enhance the system's anti-vibration capability, and incorporate emerging deep learning algorithms to pinpoint zero optical distance differences and reconstruct three-dimensional topography with greater accuracy.

3.1.3. Optical scattering method

The Optical Scattering Method is an indirect measurement technique. When light is projected onto the surface of an object, the outgoing light is modulated by the rough surface of the object. The distribution of light intensity is related to the material, roughness, and processing method of the object's surface. The inner surface roughness can be measured by establishing a relationship between the distribution of scattered light intensity and the surface roughness of the part. When a beam of light is incident on a rough surface at a certain angle, the light undergoes complex optical phenomena such as specular reflection, diffuse reflection, scattering, and diffraction on the surface, resulting in a scattered light spot within the plane as shown in Fig. 15(a)¹¹³. Bright light spots are formed in the direction of specular reflection, and two wings centered on the light spots form a scattering light band. The reflected light spot is stronger when the material surface is relatively smooth, and the scattering light band is relatively narrow. The reflected light spot is weaker if the surface is relatively rough, and the scattering light band is wider. Fig. 15(b) shows scattered light spot images of surfaces with different roughness.114

Lasers are a preferred light source for measuring surface roughness due to their excellent monochromatic, collimation, and coherence properties. In the case of large-diameter internal walls, a measurement system that combines a motion device with a sensor comprising a laser, an optoelectronic conversion module, and an analog-to-digital conversion module is typically used. Zhuang, et al. have developed a non-contact laser sensor that can inspect the internal walls of pipes. The sensor employs a laser diode light source, a halo pattern gen-

erator, and a CCD camera, and can accurately detect the inner diameter of pipes ranging from 80 mm to 160 mm with an accuracy of within 0.2 mm.

Conventional laser instruments are limited in size and unable to measure the interior of small holes. The advent of optical fibers has provided a superior solution for small-scale measurements. By using optical fibers as a propagation medium or employing optical instruments such as prisms, it is possible to alter the path of light propagation and make the measurement system more flexible in terms of optical path design. Yang, et al. 114 proposed and developed a novel fiber optic sensor that can simultaneously measure the size and surface roughness. The study investigated the effects of a fiber optic surface tilt angle and gap distance on roughness measurement. The research revealed that the center distance between the emitting and receiving fibers had the most significant impact on the sensor's effective range, while the critical angle of the receiving fiber had the greatest effect on the sensor's sensitivity.

Lu, et al. 116 have developed a fiber optic sensor measurement system using oblique light injection based on the scattering principle to detect the inner surface of a hole. The system uses a fiber optic probe that penetrates the hole for localized roughness measurement. The experimental results demonstrate that the system is suitable for measuring relatively smooth surfaces with a root-mean-square roughness value of Rq < 200. However, the probe's size limitations mean that the hole diameter being measured must be larger than 20 mm, which is not conducive to operations in narrow spaces. To address this issue, Guo and Ming¹¹⁷ proposed a fiber optic sensor roughness measurement system based on oblique scattering, capable of measuring the roughness of internal curved surfaces with a hole diameter of 4 mm or larger, as well as some narrow curved surfaces, and displaying the surface roughness value in real-time. The roughness range is between 0.5-6.3 µm, and the measurement error compared to the stylus method is less than 5%, with high accuracy, providing some reference value for roughness detection in narrow spaces. However, the measurable depth of small holes is limited to 0–5 mm, and the system is restricted by the size of the designed fiber optic sensor for measuring roughness values of deeper surfaces within the

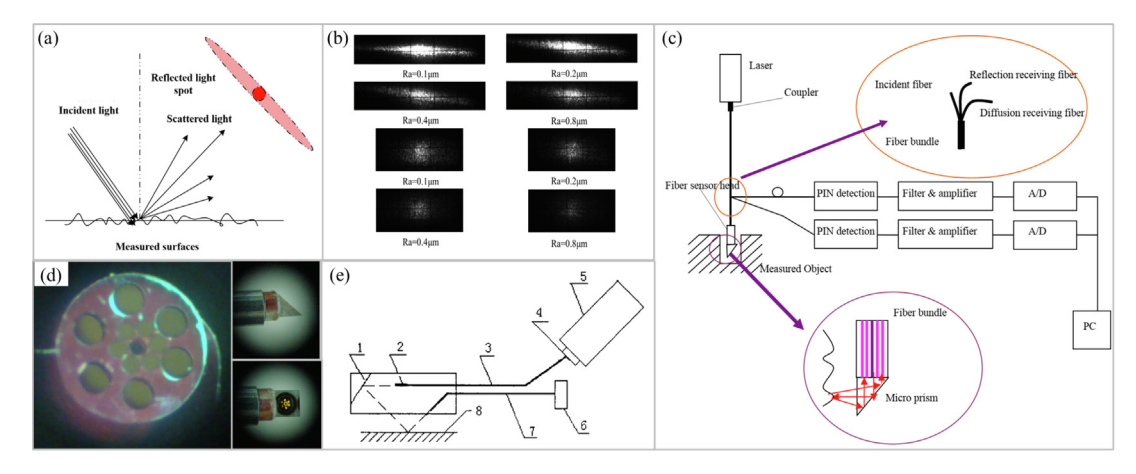


Fig. 15 (a) Scattered light band diagram of roughness surface¹¹³; (b) Scattering patterns of surfaces with different roughness; (c) Sketch map of the inner surface roughness measurement system using a fiber optic sensor¹¹⁴; (d) Pictures of the sensor head under a microscope; (e) Optical fiber sensor schematic diagram.²¹

hole. To improve measurement accuracy, Xu²¹ developed a new fiber optic sensor based on the principle of optical scattering. By adding a miniature prism with a length of 2 mm to the front end of a three-layer coaxial fiber optic bundle, it is possible to measure the roughness of the inner surface of small holes with a diameter greater than 3 mm, with a measurement accuracy ranging from 12-100 nm (Fig. 15(c)). However, the current research is limited to holes with a diameter greater than 2 mm due to the size limitations of the fiber optic material.

To sum up, the optical scattering measurement method achieves high accuracy at sub-nanometer levels. Measuring the roughness of the inner surface of precision parts requires high accuracy due to the limited space. The optical scattering method offers a relatively simple optical path and has lower requirements for the position of the workpiece during optical measurement. Additionally, the measurement system demonstrates excellent anti-interference performance, making it a primary method for measuring the surface roughness of inner wall parts. However, due to the size limitations of the measuring instrument, it is challenging to perform deep measurements on small holes below 2 mm.

3.2. Non-probing measurement

In contrast to the destructive measurement of dissected parts, the probing method is based on reducing the size of the probing tool and using the mechanical structure to probe the tool into the part to obtain internal surface topography information. However, these methods often require a high degree of stiffness and accuracy of movement of the mechanical structure, and can only be used for probing straight bores, which does not overcome the difficulty of varying curvature of complex structures such as curved pipes. Non-intrusive measurements do away with high stiffness mechanical structures and use more flexible measurement media, such as adhesive film copying, or use the laws of physics to directly detect and image internal structures, typically using methods such as X-ray CT imaging. Non-intrusive measurement allows for rapid measurement of complex internal structures with higher degrees of freedom and has developed rapidly in recent years.

3.2.1. Replica method

The replica method involves coating the workpiece surface with a replica material that has a certain degree of fluidity, ensuring it fills the microstructure of the surface to be measured under the influence of gravity or extrusion pressure. Once the replica material has solidified, it is demoulded to obtain a replica of the surface morphology. This replica is then measured and processed to indirectly obtain the original morphological information. This method is often employed to assess surface defects in complex structures such as gears and blades, as well as to measure both internal and external surface roughness. 119-121 The ability of the replica to maintain a stable structure is crucial for surface microstructure analysis, surface morphology analysis, and surface damage analysis. Common replica materials include resins, silicone rubbers, and photosensitive materials. 122–124 These materials possess the necessary fluidity and viscosity to adequately fill the microscopic peaks and valleys of a surface under gravity or external pressure. By adding catalysts and curing agents, the colloidal material can rapidly cross-link to form an elastic and flexible replica. The replication accuracy depends on the curing shrinkage rate of the material upon solidification and the elastic deformation recovery rate when demolding from the workpiece. The measurement speed primarily depends on the reaction rate of the catalyst and the cross-linking agent. A high-performance replica should exhibit high replication accuracy, good flow properties, easy release, and reliable curing, enabling fast and accurate measurement of the internal surfaces of complex structures (Fig. 16(a)).

Nilsson and Ohlsson¹²⁷ compared the measurement accuracy of three different but commonly used replication materials. The results indicate that none of the tested replica materials leave detectable traces on the original surface. All replicas achieve an accuracy within 10%, with repeatability better than 10% (excluding *Sz*). However, replicas made with Microset materials typically exhibit lower surface parameter values than the original surface. In contrast, Araldite and Technovit tend to produce some pores with a height of about 1 µm, which amplifies the *Sz* parameter ((Fig. 17)).

Microset UK's replica is a highly flexible silicone rubber compound with an ultra-high measurement accuracy of 0.1 µm. It is suitable for a wide range of applications, including surface analysis, materials research, and 3D measurement. Saxena, et al. 128 used replicas (Microset@) for indirect measurement of the circumferential surface roughness of microfabricated EDM holes. The results demonstrate that the roughness prediction accuracy of the replica technique is \pm 60 nm and \pm 50 nm for microholes with nominal diameters in the range of 0.35 mm to 0.5 mm and internal surface roughness in the range of 0.2 µm to 0.5 µm. However, the maximum aspect ratio that can be replicated is limited. For microholes with diameters of 0.35 mm and 0.5 mm, the average replication depths are approximately 2 mm and 4 mm, respectively (Fig. 18(e)). Walton, et al. 129 also evaluated and validated the measurement accuracy of Microset TM for replicating

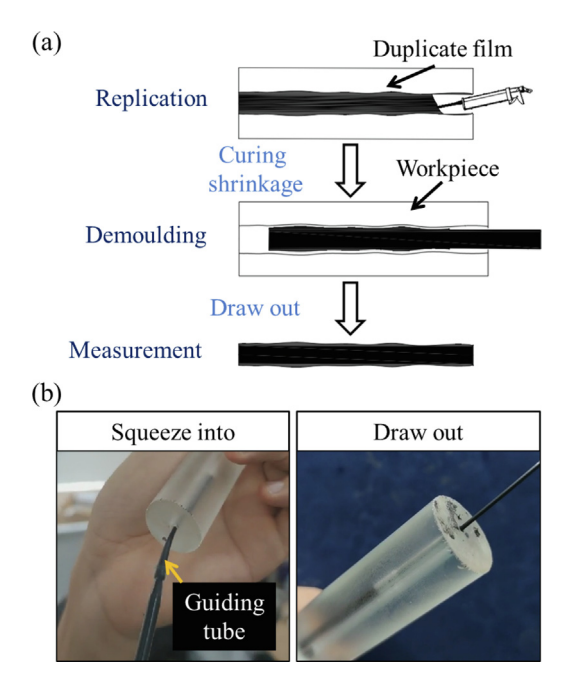


Fig. 16 Principle of replica measurement: (a) process flow, (b) physical diagram.

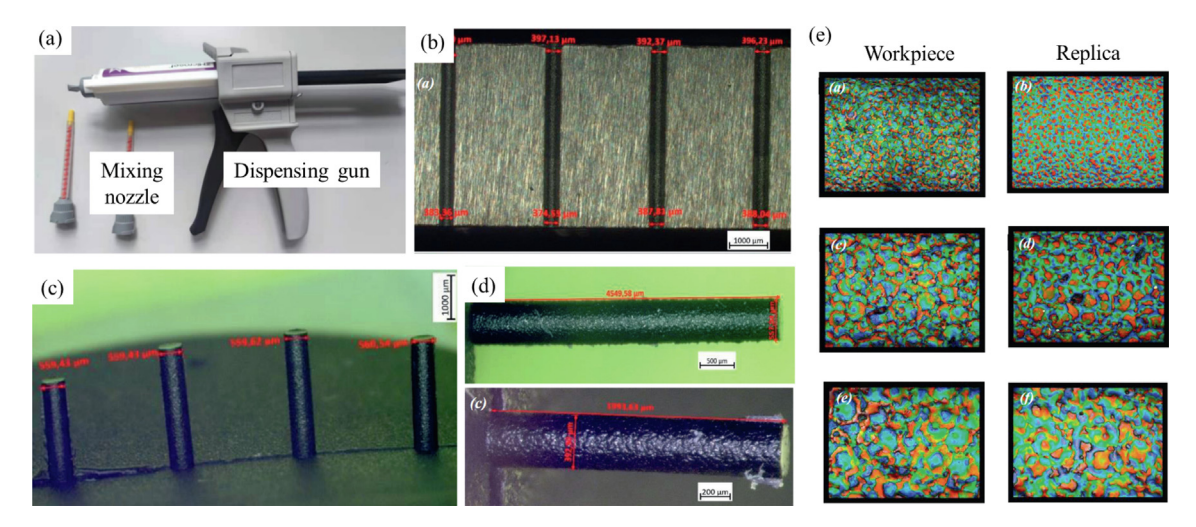


Fig. 17 Typical applications of replica measurement¹¹⁹: (a) adhesive injection tool, (b) original morphology of the microhole to be measured, (c) replicated morphology, (d) comparison between replicated and original morphology, (e) microscopic comparison between replicated and original morphology. ¹²⁸

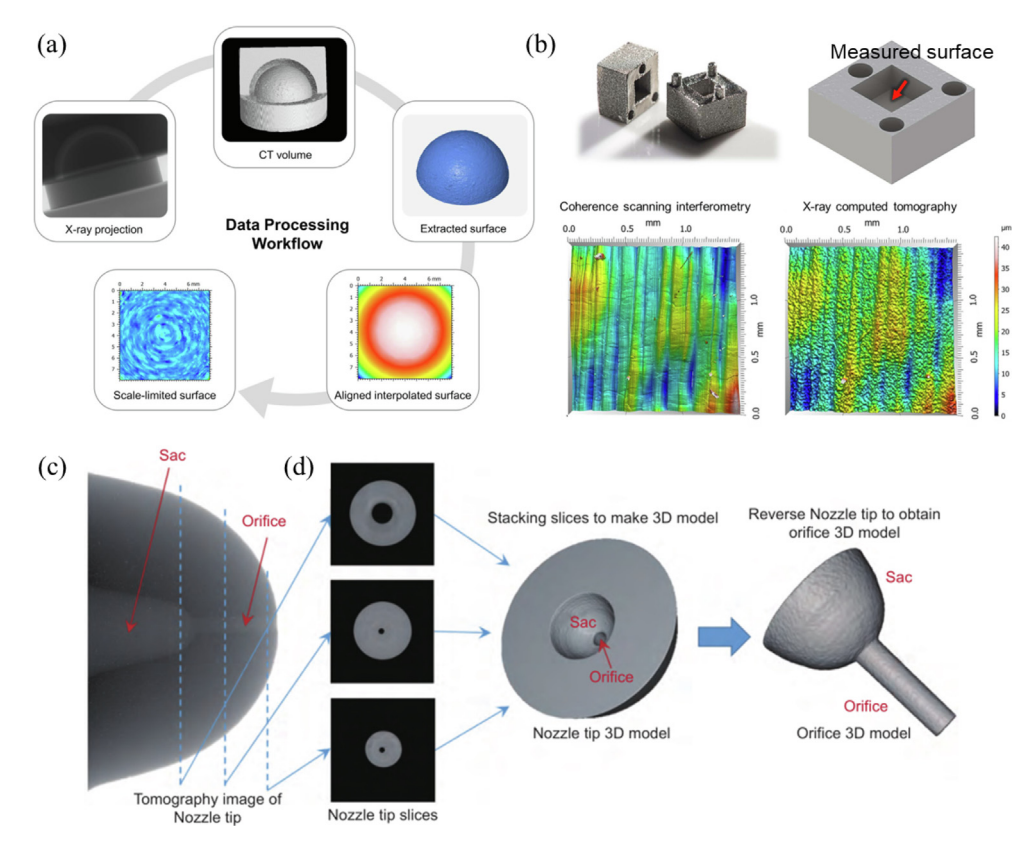


Fig. 18 (a) A flow diagram illustrating the various steps in the XCT data processing workflow ¹³¹; (b) Comparison of internal roughness measured by coherence scanning interferometry and XCT¹³⁰; (c) A typical absorption image from one set of CT scan frames and (d) the calculated slices of nozzle tip at different locations. ¹³²

the test surface of an aerofoil. The results indicate that the technique has high replication fidelity across all significant length scales. Blade chord values were accurate to 0.02%, maximum blade thickness was accurate to 2.5%, and important spatial and amplitude surface texture parameters were all accurate to within 2%.

For straight and bent tubes with simple structures, the replica method enables direct measurement and, due to the good elasticity and release properties of the replica material, facilitates rapid non-destructive testing of internal surfaces. For slender tubes with small apertures, large aspect ratios, and other complex structures like multiple channels, a flexible

mechanical structure is required to transport the replica material to the internal areas. Since the replica method does not rely on the precise movement of the mechanical structure, it only needs to ensure the smooth release of the replica material for rapid measurement.

Additionally, the replica method is suitable for retaining and comparing the surface profiles of workpieces at different stages of finishing. It also allows for the rapid and real-time copying of multiple workpieces or workpieces at various stages of finishing, which can then be brought back to the laboratory for uniform testing to observe trends in surface profiles. However, the replica method has limited accuracy, with the highest copying accuracy being 0.1 μ m, which is insufficient for measuring ultra-smooth surfaces. Moreover, the cost of the replica method is relatively high. If the replica material becomes clogged inside complex pipes, it can severely impact subsequent processing and measurement (Table 1).

3.2.2. X-ray CT method

X-ray Computed Tomography (CT) scanning measurement technology involves performing circular X-ray scans of an object to obtain information about the distribution of materials in different cross-sectional directions. This information is then used in image stitching and reconstruction algorithms to create a three-dimensional reconstruction of the object's spatial structure. As X-rays pass through the object, their energy significantly attenuates, with the degree of attenuation depending on the material type and the path taken by the X-rays. By detecting the attenuation of X-rays from different directions, it is possible to effectively distinguish the internal surface material of parts from air interfaces, thereby enhancing the resolution of three-dimensional imaging of part surface morphology, as illustrated in Fig. 18. ^{130–132}

Compared to other contact or non-contact measurement techniques, X-ray computed tomography (XCT) offers significant advantages for measuring difficult-to-reach internal surfaces, particularly in the context of the increasing application of additively manufactured complex structural components. Thompson, et al. ¹³⁰ used hollow Ti6Al4V parts produced by laser powder bed fusion as measurement workpieces to demonstrate the feasibility and potential of XCT for morphology measurement. They compared surface data sets obtained from two XCT systems with those acquired using coherent scanning interferometry and focus variation microscopy. The results indicated that XCT could provide surface information compa-

rable to traditional surface measurement techniques non-destructively, suggesting that XCT could effectively replace traditional measurement methods to some extent, especially for complex additively manufactured components.

Li, et al. 131 used synchrotron radiation X-ray micro-CT technology to evaluate the inner wall surface characteristics of micro-spray holes in fuel nozzles. Based on the threedimensional digital model of the diesel engine nozzle, they proposed a new method to unfold the hole wall surface onto a plane and conducted a quantitative evaluation of its surface characteristics. They tested and compared two single-hole nozzles using this method. The proposed measurement, based on synchrotron radiation X-ray micro-CT technology with a spatial resolution of 3.7 um, could preliminarily measure the waviness of the inner surface of the nozzles (Fig. 18(b)). Lifton, et al. 132 used XCT to non-destructively measure the internal and external surfaces of objects with micron-level spatial resolution. They designed and manufactured an additional aluminum spherical surface roughness sample and measured its surface roughness using focus variation microscopy. The sample was then XCT scanned while embedded in surrounding materials of varying thicknesses. They quantitatively and qualitatively compared the optical and XCT surface roughness measurement results, finding that the Sa value of surface roughness measurements based on XCT increased with the thickness of the surrounding material (Fig. 18(a)).

Currently, due to limitations in X-ray penetration and resolution, XCT technology cannot measure metal parts larger than a few centimeters in size. The size and materials of parts that XCT can measure are still limited. However, despite being in the early stages of development with relatively low measurement accuracy, XCT's capability to directly obtain internal interface information without being constrained by complex spatial structures demonstrates its powerful potential for measuring complex internal surface structures. This is particularly significant as the development of additive manufacturing technology makes it increasingly challenging to measure internal geometric structures.

4. Summary and future trends

4.1. Summary

The miniaturization of diameters and the increasing complexity of inner surface structures impose stringent demands on the

Table 1 Parameters	of various types of	replica materials.			
Parameter	Araldite SV40	Microset 101FF	Technovit 3040 from	Hong ye silicine 620	
Suppliers	Ciba Speciality Chemicals	Microset Products Ltd	Heraeus Kulzer GmbH	Hong ye Company, China	
Material type	Two-component epoxy resin	Silicone rubber synthetic compounds	Two-component cold curing resin based on methyl methacrylate	Condensed mold silica gel	
Appearance	Transparent	Black	Yellow	White	
Operating time /	/	4/30	4/15	30/240	
Solidification time					
Accuracy/µm	/	0.1	1	To be tested	
Hardness	,	28-30 Shore A	Indentation strength 135 N/mm ²	20 ± 2	
Shrinkage rate	,	< 0.1%	Linear shrinkage rate 1.9%	Linear shrinkage is less	
			Volume shrinkage 5.7%	than 0.3%	
Working temperature	/	−10 °C−180 °C	≤ 95 °C	Normal temperature	

accessibility of finishing and measurement technologies. This paper introduces inner surface finishing technologies from three aspects: mechanical finishing, fluid-based finishing, and energy field-assisted finishing. Additionally, internal surface measurement techniques were categorized into tool-probing and non-probing measurement. To facilitate a comprehensive comparison of these various technologies, Fig. 19, along with Tables 2 and 3, outlines the key parameters, advantages, disadvantages, and application scopes of each finishing and measurement technique.

Using finishing tools for inner surface finishing provides higher processing efficiency. Bonded abrasives, driven at high speeds by a motor, facilitate rapid material removal and converge on improving the surface roughness of the workpiece. However, these methods also generate high temperatures, scratching, and cause subsurface defects, which can lead to poor surface integrity of the part. Conversely, fluid-based finishing techniques leverage fluid to dissipate heat and utilize the flexibility of micro-scale abrasives in a fluid or semi-fluid medium, allowing them to finish narrower diameters and complex internal structures. In this approach, the pressure exerted on abrasives by the fluid is relatively low, making it easier to achieve a smooth surface at the submicron level or lower. Fig. 19 illustrates the aperture and surface quality characteristics of various internal surface finishing technologies.

Fluid-based finishing techniques show great potential, particularly for intricate internal surface structures. However, unlike mechanical finishing, fluid within a complex internal structure becomes impossible to control. Complex structures and frictional losses along the flow path inevitably cause pressure loss of fluid, resulting in inherently uneven finishing throughout the internal surface. Currently, research on fluid control within complex channels remains limited, yet this aspect is crucial for achieving uniform materials removal in complex internal surfaces.

Regarding the surface integrity of parts after finishing, mechanical finishing can cause issues such as burns, compres-

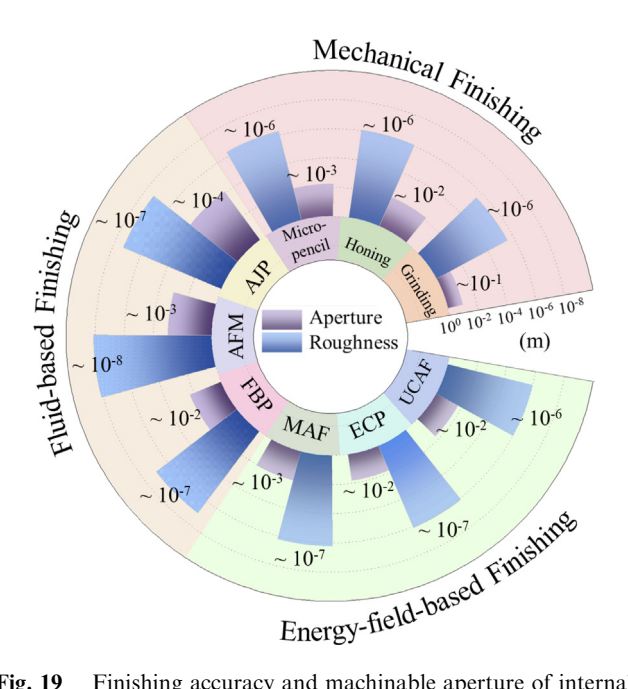


Fig. 19 Finishing accuracy and machinable aperture of internal surface finishing technology.

sive residual stress, and scratches. For fluid-based finishing techniques, common surface defects include pits, scratches, and embedded abrasive particles. In the case of AFM, the high pressure exerted by the medium on the abrasive can also induce residual compressive stress and slightly increase microhardness. For MAF, in addition to abrasive embedding, the rotary motion characteristic can lead to unavoidable circumferential marks inside the tube. For ECP, the rapid material removal, which is difficult to control, results in poor dimensional accuracy. Furthermore, impurities from other elements may be introduced on the surface during ECP. The impact of finishing on the surface integrity indices, to a certain extent, determines the application of each technique.

Table 2 summarizes the finishing methods discussed, including their parameters, advantages, disadvantages, applications, and other relevant details. Presently, AFM is relatively widely used for finishing the internal surfaces of pipelines and valves in the automotive and aerospace industries. However, AFM that require fixture adjustments and parameter modifications based on part structure struggle to meet the growing challenges posed by increasing part complexity. Energy-fieldbased finishing techniques, which are highly adaptable, can significantly enhance processing controllability and efficiency by coupling with other techniques. For instance, the combination of magnetic and ultrasonic fields with fluid finishing can modify the flow state of the fluid medium, thereby achieving higher processing efficiency and greater finishing uniformity. With the increasing complexity of parts, there is a pressing need to introduce new energy fields to minimize the impact of structure on finishing parameters.

Tool-probing measurement can achieve higher measurement accuracy, while non-probing measurement can measure more intricate structures, as shown in Table 3. Both the stylus-probing method and optical interference or scattering measurement method offer high measurement precision. Optical measurement methods, based on optical principles, provide higher measurement efficiency compared to stylus-probing method and can typically achieve global measurement. However, achieving high-precision, large-scale optical measurements require complex optical pathways, limiting their application to linear pipes. Non-probing measurements overcome the challenge of interference between the probe and complex inner surface structures, enabling flexible acquisition of surface profile information. Nonetheless, the measurement accuracy of these non-probe methods is comparatively lower.

Due to limitations in finishing and measurement methods for complex internal surface, a widely accepted standard for evaluating internal surface quality for complex structures has yet to be established. In some cases, parts are evaluated by being cut open, while in others, performance tests after finishing, such as flow resistance and heat dissipation, are conducted to determine if requirements are met. Developing standards for internal surface roughness measurements is an essential task, which could greatly advance measurement technology for internal surfaces.

4.2. Future trends

 Regarding internal surface finishing, one optimization to enhance processing accessibility is the miniaturization of tools. In mechanical finishing, the applicability of com-

Type	Key	Advantages	Limitations	Applications	Inner surface structure/aperture (mm)					
	parameters				Straight tube > 5	Straight tube < 5	Bend pipe	Multi- channel tube	Array	Micro- holes
Grinding/ Honing	Grinding speed; Honing pressure; Oilstone property.	High removal efficiency and rapid improvement of surface quality	High grinding temperature; Subsurface damage; Low accessibility.	Cylinder, valve hole, connecting rod hole, box hole, etc.	[30]	[33]				[32]
AFM	Pressure; Abrasive type; Abrasive size; number of cycles; Fixture.	High Accessibility; High Finishing Accuracy	Low Efficiency; Highly dependent on initial surface quality; Uneven material removal.	Automobile valves, fuel nozzles, turbine blades, cooling ducts, helical ducts, porous arrays, etc.	[42]	[44]	[47]	[46]		[48]
AJP	Abrasive type; Abrasive size; Jet velocity.	Suitable for small hole; No abrasive blockage.	Low processing efficiency; Unable to finish complex structure	Fuel nozzle, needle, aluminum and other metal pipes	[50]		[51]			[92]
FBP	Abrasive type; Abrasive size; Fluidization velocity	High processing efficiency, suitable for industrial mass production	Embedded abrasive; Unable to finish complex structure.	Bolt, piston rod, and other simple straight and short pipes	[58]					
ECP	Current; Voltage; Temperature; Liquid composition	Not limited by the mechanical properties of the workpiece; High Efficiency;	Not suitable for non- conductive materials; Difficult to control the geometric accuracy; Environmental pollution	Cardiovascular stents, additive manufacturing inner holes and array structures, metal pipes	[80]	[83]	[85]		[89]	
MAF	Magnetic intensity; Abrasive size; Rotate speed;	Self-adaptive to the surface structure; High finishing accuracy	Not suitable for non-rotationally symmetric parts; High requirements for the preparation of magnetic particles.	Needle tubes, fuel injection rods, copper tubes, etc.	[65]	[72]	[75]			[69]
UCAF	Abrasive type; Abrasive size; Ultrasonic amplitude	Commonly used as an auxiliary method to enhance the kinetic energy of the abrasives	High equipment requirements; Lack of stability in processing.	Simple additive manufacturing inner pipe and channels	[53]	[54]				

plex structural parts can be enhanced by reducing tool size and increasing the flexibility of the drive shaft. Research efforts could investigate the feasibility of using flexible shafts or coated wires to access narrow internal cavities and finish surfaces effectively.

(2) By utilizing additive manufacturing technology, components in high-end equipment, such as aero-engine fuel injectors, are evolving towards greater integration and lightweight designs. Post-processing for these components has become a common challenge in modern indus-

Туре	Measuring range	Measuring speed	Measuring accuracy	Measuring aperture	Measuring DOF	Reference
Optical interference	Global	$\triangle \triangle \triangle \triangle \triangle$	ል ል ል ል ል	>10 mm	☆	125,127
Optical scattering	Global	**	& &	> 5 mm	**	131,132
X-ray CT	Global	☆☆☆☆	☆	Unlimited	***	139,141
Stylus-probing	Line	☆	☆☆☆☆	≥0.1 mm	☆	115,119
Replica method	Local	$^{\circ}$	**	> 1 mm	$^{\circ}$	135,136

try. Fluid-based finishing technology stands out as one of the most promising solutions. However, its controllability is currently limited in achieving uniform material removal. Advancing the controllability of the fluid medium to allow for highly controlled material removal on internal surfaces should be a priority in subsequent studies.

- (3) Multi-field assisted finishing technologies can effectively enhance processing quality and efficiency. Nonetheless, the coupling and synergistic mechanisms of multiple energy fields lack sufficient insight, and the interactions between these energy fields can lead to unpredictable processing outcomes. In-depth research into the coupling effects of various energy fields is essential to achieving optimal finishing results. Future investigations could leverage molecular dynamics simulations and similar methods to clarify the mechanisms of multi-field interactions.
- (4) Regarding internal surface roughness measurement, the miniaturization of measurement systems is also a key research focus. Optimization strategies could include reducing the size of optical prisms, utilizing fiber optic sensors, optimizing optical path designs to lower the number of prisms, increasing the resolution of photoelectric sensors, and refining extraction algorithms. These measures aim to minimize the optical path size while enhancing both measurement accuracy and efficiency.
- (5) As internal surface structures become narrower and more complex, demand for small-diameter flexible measurement technologies, such as fiber optic endoscopes, is increasing. However, these technologies is prone to face challenges in measuring complex pipes with multiple curvatures. In contrast, non-contact measurement techniques, such as X-ray CT, naturally overcome these limitations posed by complex structures. Future work can focus on improving the resolution of these measurement techniques, which show broad application prospects.

CRediT authorship contribution statement

Jiang GUO: Supervision, Resources, Methodology. Qikai LI: Writing – original draft, Investigation. Pu QIN: Writing – review & editing. Ankang YUAN: Writing – original draft. Mingyang LU: Writing – original draft. Xiaolong KE: Visualization. Yicha ZHANG: Visualization. Benny C.F. CHEUNG: Visualization.

Declaration of competing interest

The authors declare that they have no known competing financial interests or personal relationships that could have appeared to influence the work reported in this paper.

Acknowledgements

The authors would like to acknowledge the financial supports from National Key R&D Program of China (No. 2022YFB3403301) and the Funds for International Cooperation and Exchange of the National Natural Science Foundation of China (No. 52311530080).

References

- 1. Faghri A. Review and advances in heat pipe science and technology. *J Heat Transfer* 2012;**134**(12):123001.
- Li W, Zhou P, Lin W-C, et al. Effects of needle inner surface topography on friction and biopsy length. *Int J Mech Sci* 2016;119:412–8.
- 3. Kim B, Park S. Study on in-nozzle flow and spray behavior characteristics under various needle positions and length-to-width ratios of nozzle orifice using a transparent acrylic nozzle. *Int J Heat Mass Transf* 2019;**143**.
- 4. Chen Y, Wang X, Zhang C. Polishing processing to internal surface of non-magnetic pipe by magnetic abrasive finishing. *Trans Tech Publ* 2008:137–40.
- Wan S, Ang YJ, Sato T, et al. Process modeling and CFD simulation of two-way abrasive flow machining. Int J Adv Manuf Tech 2013;71(5–8):1077–86.
- Yamaguchi M, Furumoto T, Inagaki S, et al. Internal face finishing for a cooling channel using a fluid containing free abrasive grains. *Int J Adv Manuf Technol* 2021;114(1– 2):497–507.
- Yang C, Su H, Gao S, et al. Surface quality and geometric accuracy control of fuel nozzle single-pass honing. *Int J Adv Manuf Tech* 2021;114(11–12):3325–36.
- 8. Ren N, Yu Y, Li H. Improved roughness measurement method using fiber Bragg gratings and machine learning. *Sens Actuators*, A 2021;332.
- Liu G, Li J, Zhu S, et al. Experimental and numerical analysis
 of the assisted abrasive flow of magnetic particles on the
 polishing of fuel injection nozzles. *Magnetochemistry* 2022;8
 (3):35.
- Li J, Dong X, Liu Y, et al. Quality research and prediction of six-order variable-diameter pipe processed by solid-liquid twophase magnetic abrasive flow. *Int J Adv Manuf Tech* 2021;114 (11–12):3763–78.
- Guo J, Song C, Fu Y, et al. Internal surface quality enhancement of selective laser melted inconel 718 by abrasive flow machining. J Manuf Sci E-T ASME 2020;142(10):101003.

- Rosa B, Mognol P, Hascoët J-Y. Laser polishing of additive laser manufacturing surfaces. J Laser Appl 2015;27(S2):S29102.
- Davoodi F, Taghian M, Carbone G, et al. An overview of the latest progress in internal surface finishing of the additively manufactured metallic components. *Materials (Basel)* 2023;16 (10):3867.
- Malakizadi A, Mallipeddi D, Dadbakhsh S, et al. Postprocessing of additively manufactured metallic alloys - A review. *Int J Mach Tool Manu* 2022;179:103908.
- Dong G, Lang C, Li C, et al. Formation mechanism and modelling of exit edge-chipping during ultrasonic vibration grinding of deep-small holes of microcrystalline-mica ceramics. *Ceram Int* 2020;46(8):12458–69.
- Li S, Wang L, Li G, et al. Small hole drilling of Ti-6Al-4V using ultrasonic-assisted plasma electric oxidation grinding. *Precis Eng* 2021;67:189–98.
- Kiani A, Esmailian M, Amirabadi H. Abrasive flow machining: a review on new developed hybrid AFM process. *Int J adv Des Manuf Technol* 2016;9(1):61–71.
- Kumar R, Komma VR. Recent advancements in magnetic abrasive finishing: a critical review. Eng Res Express 2024;6 (1):012504.
- Mu J, Sun T, Leung CLA, et al. Application of electrochemical polishing in surface treatment of additively manufactured structures: a review. *Prog Mater Sci* 2023;136:101109.
- Peiner E, Balke M, Doering L. Form measurement inside fuel injector nozzle spray holes. *Microelectron Eng* 2009;86(4–6):984–6.
- **21.** Xu X, Liu S, Hu H. A new fiber optic sensor for inner surface roughness measurement. *SPIE* 2009:149–57.
- Tan KL, Yeo S-H, Ong CH. Nontraditional finishing processes for internal surfaces and passages: a review. *Proc Inst Mech Engineers Part B-J Eng Manuf* 2017;231(13):2302–16.
- Bedi TS, Rana AS. Surface finishing requirements on various internal cylindrical components: a review. *J Micromanuf* 2021;4 (2):216–28.
- 24. Lee J-Y, Nagalingam AP, Yeo SH. A review on the state-ofthe-art of surface finishing processes and related ISO/ASTM standards for metal additive manufactured components. *Virtual Phys Prototyping* 2021;**16**(1):68–96.
- 25. Fang F. Advances in polishing of internal structures on parts made by laserbased powder bed fusion. Front Mech Eng 2023;18(1):8.
- Peiner E, Balke M, Doering L. Slender tactile sensor for contour and roughness measurements within deep and narrow holes. *IEEE Sens J* 2008;8(12):1960–7.
- Jiao F, Liu L, Cheng W, et al. Review of optical measurement techniques for measuring three-dimensional topography of inner-wall-shaped parts. *Measurement* 2022;202:111794.
- 28. Sedghi R, Shahbeik H, Rastegari H, et al. Turning biodiesel glycerol into oxygenated fuel additives and their effects on the behavior of internal combustion engines: a comprehensive systematic review. *Renew Sust Energ Rev.* 2022;167:112805.
- Xiao W, Zi Y, Chen B, et al. A novel approach to machining condition monitoring of deep hole boring. *Int J Mach Tool Manu* 2014;77:27–33.
- **30.** Brinksmeier E, Mutlugünes Y, Klocke F, et al. Ultra-precision grinding. *CIRP Ann* 2010;**59**(2):652–71.
- 31. Aurich JC, Engmann J, Schueler GM, et al. Micro grinding tool for manufacture of complex structures in brittle materials. *CIRP Ann* 2009;**58**(1):311–4.
- Aurich JC, Carrella M, Walk M. Micro grinding with ultra small micro pencil grinding tools using an integrated machine tool. CIRP Ann 2015;64(1):325–8.
- Dong G, Zhang L. Investigation on grinding force and machining quality during rotary ultrasonic grinding deepsmall hole of fluorophlogopite ceramics. *Int J Adv Manuf Tech* 2019;104(5–8):2815–25.

- Zhu X, Liu Y, Zhang J, et al. Ultrasonic-assisted electrochemical drill-grinding of small holes with high-quality. J Adv Res 2020;23:151–61.
- 35. Pawlus P, Reizer R. Functional importance of honed cylinder liner surface texture: a review. *Tribol Int* 2022;**167**:107409.
- Pan L, Zhu L. Preliminary study on mechanism of superalloy deep-hole honing technology. *Appl Mech Mater* 2012;271– 272:353–6.
- Yang C, Su H, Gao S, et al. Characterization and life prediction of single-pass honing tool for fuel injection nozzle. *Chin J Aeronaut* 2021;34(4):225–40.
- Barros GHC, Schramm CR, Franco SD, et al. Effect of grain size and number of strokes on Rk parameters and emptiness coefficient in honing process. *Int J Adv Manuf Tech* 2019;103(9– 12):3717–34.
- Arantes LJ, Fernandes KA, Schramm CR, et al. The roughness characterization in cylinders obtained by conventional and flexible honing processes. *Int J Adv Manuf Tech* 2017;93(1– 4):635–49.
- Petare AC, Jain NK. A critical review of past research and advances in abrasive flow finishing process. *Int J Adv Manuf Tech* 2018:97(1–4):741–82.
- Singh S, Kumar H, Kumar S, et al. A systematic review on recent advancements in Abrasive Flow Machining (AFM). *Mater Today Proc* 2022;56:3108–16.
- 42. Singh S, Sankar MR. Design and performance evaluation of abrasive flow finishing process during finishing of stainless steel tubes. *Mater Today Proc* 2015;2(4–5):3161–319.
- Singh S, Sankar MR. Rheological study of the developed medium and its correlation with surface roughness during abrasive flow finishing of micro-slots. *Mach Sci Technol* 2020;24(6):882–905.
- 44. Liu G, Zhang X, Zang X, et al. Study on whole factorial experiment of polishing the micro-hole in non-linear tubes by abrasive flow. Adv. Mech Eng. 2018;10(8):1687814018794590.
- 45. Li J, Qu J, Lu H, et al. Effectiveness analysis of abrasive flow polishing S-shaped elbow with side holes based on large eddy simulation. *Int J Adv Manuf Tech* 2021;115(11–12):3887–906.
- 46. Han S, Salvatore F, Rech J, et al. Abrasive flow machining (AFM) finishing of conformal cooling channels created by selective laser melting (SLM). *Precis Eng* 2020;64:20–33.
- Kum CW, Wu CH, Wan S, et al. Prediction and compensation of material removal for abrasive flow machining of additively manufactured metal components. J Mater Process Technol 2020;282:116704.
- 48. Li J, Wang X, Hu J, et al. Optimisation design and analysis of variable-diameter pipe parameters for solid–liquid two-phase abrasive flow processing. *J Eng* 2020;**2020**(14):985–91.
- Shi CY, Yuan JH, Wu F, et al. Study on submerged jet problem of concave optics surface in fluid jet polishing. Adv Mat Res 2011;308–310:923–7.
- Cheung CF, Wang CJ, Cao ZC, et al. Development of a multi jet polishing process for inner surface finishing. Precis Eng-J Int Soc Precis Eng Nanotechnol 2018;52:112–21.
- Furumoto T, Ueda T, Amino T, et al. A study of internal face finishing of the cooling channel in injection mold with free abrasive grains. J Mater Process Technol 2011;211 (11):1742–2178.
- Deng Q, Wang Y, Sun L, et al. A polishing method using selfexcited oscillation abrasive flow for the inner surface of workpiece. *Int J Adv Manuf Technol* 2022;119(5–6):4093–108.
- Nagalingam AP, Lee J-Y, Yeo SH. Multi-jet hydrodynamic surface finishing and X-ray computed tomography (X-CT) inspection of laser powder bed fused Inconel 625 fuel injection/ spray nozzles. J Mater Process Technol 2021;291:117018.
- 54. Nagalingam AP, Yeo SH. Surface finishing of additively manufactured Inconel 625 complex internal channels: A case

study using a multi-jet hydrodynamic approach. *Addit Manuf* 2020;36:101428.

- 55. Gu Q, Zhang Z, Zhou H, et al. A novel approach of jet polishing for interior surface of small-grooved components using three developed setups. *Int J Extreme Manuf* 2024;6 (2):025101.
- Barletta M. A new technology in surface finishing: fluidized bed machining (FBM) of aluminium alloys. J Mater Process Technol 2006;173(2):157–65.
- Barletta M, Guarino S, Rubino G, et al. Progress in fluidized bed assisted abrasive jet machining (FB-AJM): internal polishing of aluminium tubes. *Int J Mach Tool Manuf* 2007;47(3-4):483-95.
- Barletta M, Tagliaferri V. Development of an abrasive jet machining system assisted by two fluidized beds for internal polishing of circular tubes. *Int J Mach Tool Manuf* 2006;46(3– 4):271–83.
- Barletta M, Ceccarelli D, Guarino S, et al. Fluidized bed assisted abrasive jet machining (FB-AJM): precision internal finishing of Inconel 718 components. *J Manuf Sci Eng* 2007;129 (6):1045–59.
- Barletta M. Progress in abrasive fluidized bed machining. Article; Proceedings Paper. J Mater Process Technol 2009;209 (20):6087–102.
- Sun X, Zou Y. Development of magnetic abrasive finishing combined with electrolytic process for finishing SUS304 stainless steel plane. Int J Adv Manuf Tech 2017;92(9):3373–84.
- Yan Z, Yang S, Li Y, et al. Magnetic field-assisted finishing: mechanism, application, and outlook. *Int J Adv Manuf Tech* 2023;131(5–6):2719–58.
- 63. Wang L, Sun Y, Chen F, et al. Experimental study on vibration-assisted magnetic abrasive finishing for internal blind cavity by bias external rotating magnetic pole. *Precis* Eng-J Int Soc Precis Eng Nanotechnol 2022;74:69–79.
- Verma GC, Kala P, Pandey PM. Experimental investigations into internal magnetic abrasive finishing of pipes. *Int J Adv Manuf Technol* 2017;88(5–8):1657–68.
- Yamaguchi H, Shinmura T. Internal finishing process for alumina ceramic components by a magnetic field assisted finishing process. *Precis Eng-J Int Soc Precis Eng Nanotechnol* 2004;28(2):135–42.
- 66. Guo J, Au KH, Sun C-N, et al. Novel rotating-vibrating magnetic abrasive polishing method for double layered internal surface finishing. J Mater Process Technol 2019;264:422–37.
- 67. Yun H, Han B, Chen Y, et al. Internal finishing process of alumina ceramic tubes by ultrasonic-assisted magnetic abrasive finishing. Int J Adv Manuf Technol 2016;85(1-4):727-34.
- Singh G, Kumar H, Kansal HK. Investigations into internal roundness of Inconel 625 tubes with chemically assisted magnetic abrasive finishing. *Mater Today: Proc* 2019;33:1579–85.
- Yamaguchi H, Shinmura T, Ikeda R. Study of internal finishing of austenitic stainless steel capillary tubes by magnetic abrasive finishing. *J Manuf Sci Eng* 2007;129(5):885–92.
- Yamaguchi H, Shinmura T, Sekine M. Uniform internal finishing of SUS304 stainless steel bent tube using a magnetic abrasive finishing process. *J Manuf Sci Eng* 2005;127(3):605–11.
- Yamaguchi H, Kang J, Hashimoto F. Metastable austenitic stainless steel tool for magnetic abrasive finishing. CIRP Ann 2011;60(1):339–42.
- Kang J, Yamaguchi H. Internal finishing of capillary tubes by magnetic abrasive finishing using a multiple pole-tip system. *Precis Eng* 2012;36(3):510–6.
- Kang J, George A, Yamaguchi H. High-speed internal finishing of capillary tubes by magnetic abrasive finishing. *Procedia* CIRP 2012;1:414–8.

 Nteziyaremye V, Wang Y, Li W, et al. Surface finishing of needles for high-performance biopsy. *Procedia CIRP* 2014:14:48–53.

- 75. Deng Y, Zhao Y, Zhao G, et al. Study on magnetic abrasive finishing of the inner surface of Ni–Ti alloy cardiovascular stents tube. *Int J Adv Manuf Tech* 2021;**118**(7–8):2299–309.
- Yu Z, Han B, Chen S, et al. Study on the inner surface finishing of irregular spatial elbow pipe by the centerline reconstruction. *Int J Adv Manuf Technol* 2017;93(9–12):3085–93.
- 77. Allen RP, Arrowsmith HW, Charlot LA, et al. Electropolishing as a decontamination process: progress and applications; 1978.
- 78. Han W, Fang F. Fundamental aspects and recent developments in electropolishing. *Int J Mach Tool Manuf* 2019;**139**:1–23.
- Schmickler W. Electronic effects in the electric double layer. Chem Rev 1996;96(8):3177–200.
- Fayazfar H, Rishmawi I, Vlasea M. Electrochemical-based surface enhancement of additively manufactured Ti-6Al-4V complex structures. J Mater Eng Perform 2021;30(3):2245–55.
- 81. Ali U, Fayazfar H, Ahmed F, et al. Internal surface roughness enhancement of parts made by laser powder-bed fusion additive manufacturing. *Vacuum* 2020;177:109314.
- Zhao C, Qu N, Tang X. Removal of adhesive powders from additive-manufactured internal surface via electrochemical machining with flexible cathode. *Precis Eng* 2021;67:438–52.
- An L, Wang D, Zhu D. Combined electrochemical and mechanical polishing of interior channels in parts made by additive manufacturing. *Addit Manuf* 2022;51:102638.
- 84. Wang Y, Wei X, Li Z, et al. Experimental investigation on the effects of different electrolytic polishing solutions on nitinol cardiovascular stents. J Mater Eng Perform 2021;30 (6):4318–27.
- 85. Chang S, Liu A, Ong CYA, et al. Highly effective smoothening of 3D-printed metal structures via overpotential electrochemical polishing. *Mater Res Lett* 2019;7(7):282–9.
- Mohammad AEK, Wang D. Electrochemical mechanical polishing technology: recent developments and future research and industrial needs. *Int J Adv Manuf Tech* 2016;86(5):1909–24.
- 87. Kim S-H, Choi S-G, Choi W-K, et al. A study of the improvement surface roughness and optimum machining characteristic of L-shaped tube STS 316L by electropolishing. *Int J Adv Manuf Tech* 2015;85(9–12):2313–24.
- 88. Zhao C, Qu N, Tang X. Confined electrochemical finishing of additive-manufactured internal holes with coaxial electrolyte flushing. *J Electrochem Soc.* 2021;168(11):113504.
- 89. Pyka G, Burakowski A, Kerckhofs G, et al. Surface modification of Ti6Al4V open porous structures produced by additive manufacturing. Adv Eng Mater 2012;14(6):363-70.
- Gomez-Gallegos AA, Mill F, Mount AR. Surface finish control by electrochemical polishing in stainless steel 316 pipes. J Manuf Process 2016;23:83–9.
- 91. Guo J, Li Q, Tong Z, et al. A new internal surface polishing method for sub-millimeter slender tube with varying diameters. *CIRP Ann* 2024;73(1):265–8.
- Guo J, Qin P, Li Q, et al. A new magnetic enhanced chemical mechanical polishing method for quartz glass slender holes. J Mater Process Technol 2024;327:118361.
- Zhao C, Qu N, Tang X. Electrochemical mechanical polishing of internal holes created by selective laser melting. *J Manuf Process* 2021;64:1544–62.
- Tan KL, Yeo SH. Surface finishing on IN625 additively manufactured surfaces by combined ultrasonic cavitation and abrasion. *Addit Manuf* 2020;31.
- Abbott EJ, Firestone FA. Apparatus for determining roughness of surfaces. United States patent US 2048154. 1936 Jul 21.
- 96. Çalışkan E, İpek SK, Seisoğlu A, et al. Characteristics of surface properties of aluminum flat products related with different

- annealing temperature and cleaning properties. Springer. p. 323-9.
- Zhang RJ, Tang L, Zheng Z. Novel instrument for automatic measuring roughness of deep hole surface based on ARM920T circuit block. Opt Precis Eng 2008(05):912–6 [Chinese].
- Lebrasseur E, Pourciel J-B, Bourouina T, et al. A new characterization tool for vertical profile measurement of highaspect-ratio microstructures. *J Micromech Microeng* 2002;12 (3):280.
- Peiner E, Doering L, Balke M, et al. Silicon cantilever sensor for micro-/nanoscale dimension and force metrology. *Microsyst Technol* 2008;14:441–51.
- Peiner E, Doering L. MEMS cantilever sensor for nondestructive metrology within high-aspect-ratio micro holes. *Microsyst Technol* 2010;16:1259–68.
- Peiner E, Doering L. Nondestructive evaluation of diesel spray holes using piezoresistive sensors. *IEEE Sens J* 2012;13 (2):701–8.
- 102. Xu M, Kauth F, Mickan B, et al. Traceable profile and roughness measurements inside micro sonic nozzles with the Profilscanner. EDP. Sciences 2015:13004.
- 103. Doering L, Brand U, Bütefisch S, et al. High-speed microprobe for roughness measurements in high-aspect-ratio microstructures. Meas Sci Technol 2017;28(3):034009.
- 104. Wasisto HS, Yu F, Doering L, et al. Fabrication of wearresistant silicon microprobe tips for high-speed surface roughness scanning devices. SPIE 2015;9517:536–42.
- 105. Brand U, Xu M, Doering L, et al. Long slender piezo-resistive silicon microprobes for fast measurements of roughness and mechanical properties inside micro-holes with diameters below 100 μm. Sensors 2019;19(6):1410.
- 106. Xu M, Li Z, Fahrbach M, et al. Investigating the trackability of silicon microprobes in high-speed surface measurements. Sensors 2021;21(5):1557.
- 107. Cui K, Liu Q, Huang X, et al. Scanning error detection and compensation algorithm for white-light interferometry. Opt Lasers Eng 2022;148:106768.
- 108. Jiao F, Liu L, Cheng W, et al. Review of optical measurement techniques for measuring three-dimensional topography of inner-wall-shaped parts. *Measurement* 2022:111794.
- 109. Li M, Study on measuring method of microtopography of inner wall surface of narrow tubular optical element [dissertation]. Mianyang: China Academy of Engineering Physics, 2022 [Chinesel.
- 110. Gao H, Zhang X, Fang F. Interferometry of a reflective axicon surface with a small cone angle using an optical inner surface. *Meas Sci Technol* 2017;28(9):095204.
- 111. Dong Y, Li Z, Zhu L, et al. Topography measurement and reconstruction of inner surfaces based on white light interference. *Measurement* 2021;**186**:110199.
- 112. Albertazzi G, Viotti M, Dal Pont A. A white-light interferometer for inner cylindrical surfaces. 2006:62930F.
- 113. Cai W, Research of surface roughness measurement system based on laser scattering [dissertation]. Wuhan: Huazhong University of Science & Technology, 2020 [Chinese].
- 114. Yang Y, Yamazaki K, Aoyama H, et al. Fiber optic surface topography measurement sensor and its design study. *Precis* Eng 2000;24(1):32–40.

- Zhuang BH, Zhang W, Cui DY. Noncontact laser sensor for pipe inner wall inspection. Opt Eng 1998;37(5):1643-7.
- Lu D, Yuan F, Cheng Z. Measurement of roughness inside aperture. The 2nd international symposium on instrument science and technology; 2002:5.
- 117. Guo C, Ming Y. Analysis of measuring curved surface roughness method based on oblique laser scattering style. J Mech Electric Eng 2014;31(12):1535–40.
- 118. Sun X, Research on the measurement of the roughness of the inner surface of thin rods based on the light scattering method [dissertation]. Harbin: Harbin Institute of Technology, 2011 [Chinese].
- Shilpa MK, Yendapalli V. Surface roughness estimation techniques for drilled surfaces: a review. *Mater Today Proc* 2022;52:1082–91.
- Xu C, Reece C, Kelley M. Characterization of Nb SRF cavity materials by white light interferometry and replica techniques. *Appl Surf Sci* 2013;274:15–21.
- Ivanov T, Bührig-Polaczek A, Vroomen U, et al. Replication of specifically microstructured surfaces in A356-alloy via lost wax investment casting. *J Micromech Microeng* 2011;21(8):085026.
- 122. Zhou W, Tang J, Chen H, et al. A comprehensive investigation of plowing and grain-workpiece micro interactions on 3D ground surface topography. *Int J Mech Sci* 2018;144:639–53.
- 123. Bassoli E, Denti L. Investigation on the effectiveness of through-hole replicas of deep small holes. *Manuf Technol* 2018:18(3):357–62.
- 124. Lutey AHA, Lazzini G, Gemini L, et al. Insight into replication effectiveness of laser-textured micro and nanoscale morphology by injection molding. *J Manuf Process* 2021;**65**:445–54.
- 125. Jolivet S, Mezghani S, El Mansori M. Multiscale analysis of replication technique efficiency for 3D roughness characterization of manufactured surfaces. Surf Topogr Metrol Prop 2016;4(3):035002.
- Goodall RH, Darras LP, Purnell MA. Accuracy and precision of silicon based impression media for quantitative areal texture analysis. Sci Rep 2015;5:10800.
- Nilsson L, Ohlsson R. Accuracy of replica materials when measuring engineering surfaces. *Int J Mach Tool Manu* 2001;41 (13):2139–45.
- 128. Saxena KK, Bellotti M, Qian J, et al. Characterization of circumferential surface roughness of micro-EDMed holes using replica technology. *Procedia CIRP* 2018;68:582–7.
- 129. Walton K, Fleming L, Goodhand M, et al. High fidelity replication of surface texture and geometric form of a high aspect ratio aerodynamic test component. Surf Topogr Metrol Prop 2016;4(2):025003.
- Thompson A, Senin N, Maskery I, et al. Internal surface measurement of metal powder bed fusion parts. *Addit Manuf* 2018;20:126–33.
- 131. Li Z, Zhao W, Wu Z, et al. The measurement of internal surface characteristics of fuel nozzle orifices using the synchrotron Xray micro CT technology. Sci China Technol Sci 2018;61 (11):1621–7.
- 132. Lifton JJ, Liu Y, Tan ZJ, et al. Internal surface roughness measurement of metal additively manufactured samples via x-ray CT: the influence of surrounding material thickness. *Surf Topogr Metrol Prop* 2021;9(3):035008.